

MEMORANDUM

RM-5442-PR

FEBRUARY 1968

BACKSCATTER LIMITATIONS IN
ACTIVE NIGHT-VISION SYSTEMS

H. Steingold and R. E. Strauch

PREPARED FOR:

UNITED STATES AIR FORCE PROJECT RAND

The **RAND** *Corporation*
SANTA MONICA • CALIFORNIA

MEMORANDUM

RM-5442-PR

FEBRUARY 1968

**BACKSCATTER LIMITATIONS IN
ACTIVE NIGHT-VISION SYSTEMS**

H. Steingold and R. E. Strauch

This research is supported by the United States Air Force under Project RAND — Contract No. F44620-67-C-0045 — monitored by the Directorate of Operational Requirements and Development Plans, Deputy Chief of Staff, Research and Development, Hq USAF. RAND Memoranda are subject to critical review procedures at the research department and corporate levels. Views and conclusions expressed herein are nevertheless the primary responsibility of the author, and should not be interpreted as representing the official opinion or policy of the United States Air Force or of The RAND Corporation.

DISTRIBUTION STATEMENT

Distribution of this document is unlimited.

The **RAND** *Corporation*

1700 MAIN ST. • SANTA MONICA • CALIFORNIA • 90406

PREFACE

This Memorandum, prepared as part of RAND's continuing study of night-vision devices, considers one of the fundamental limitations on the usefulness of active night-viewing systems—backscatter. It is particularly applicable to airborne tactical systems for night attack. The well-defined and relatively realistic mathematical model presented may be used to determine range limitations of existing or proposed systems. The study provides a guideline for those considering system feasibility.

SUMMARY

A fundamental limitation in using an artificial source of illumination for night viewing is backscatter by the atmosphere. This Memorandum explores that limitation. A mathematical model of an active night vision system is constructed, and formulas for the signal received from a target and the backscatter caused by the intervening atmosphere are derived. Signal-to-noise ratio is defined, and its use as a measure of system performance is discussed. Several hypothetical systems are defined and graphs of the signal-to-noise ratio as a function of range are presented. Additional graphs show the power which would be required by the systems to achieve a given signal-to-noise ratio as a function of range.

CONTENTS

PREFACE	iii
SUMMARY	v
Section	
I. INTRODUCTION	1
II. FUNCTIONAL MODEL AND THEORETICAL DERIVATIONS. .	3
Backscatter	6
Derivation of f	7
Gated Systems	10
Evaluation of Performance	14
III. EFFECTS OF SYSTEM PARAMETERS ON SIGNAL-TO-NOISE RATIO	21
IV. ILLUSTRATIVE SYSTEMS	25
V. COMPUTATIONAL RESULTS AND CONCLUSIONS	31
REFERENCES	53

I. INTRODUCTION

A fundamental limitation in using an artificial source of illumination for night viewing is backscatter by the atmosphere. Most people have experienced the effects of backscatter when driving in a fog. The usefulness of automobile headlights is reduced by both fog-caused attenuation and backscatter. High beams are affected more than low beams, because more of the high beam passes through the driver's field of view, and he sees correspondingly more of the backscatter. Backscatter can be reduced by the use of yellow fog lights mounted below the ordinary headlights. Yellow light is scattered less than shorter wavelength light, and the lower position of the fog lights results in less of the backscatter falling within the driver's field of view. Since auto headlights do not have to provide extreme long-range viewing, backscatter does not seriously limit their effectiveness in good weather. However, in the design of systems having appreciably greater viewing range than is required of auto headlights, backscatter may even then become a limiting factor in system performance. For example, range considerations usually predominate in the selection of an airborne night-vision system for military applications.

In this Memorandum, a mathematical model of an active night-vision system is constructed, and formulas for the

signal received from a target and the backscatter caused by the intervening atmosphere are derived. Signal-to-noise ratio is defined, and the advantages and disadvantages of using signal-to-noise ratio as a measure of system performance are discussed. Some conclusions are drawn directly from the model. The model is then applied to several hypothetical systems felt to be representative of airborne systems and signal-to-noise ratio curves are obtained.

II. FUNCTIONAL MODEL AND THEORETICAL DERIVATIONS

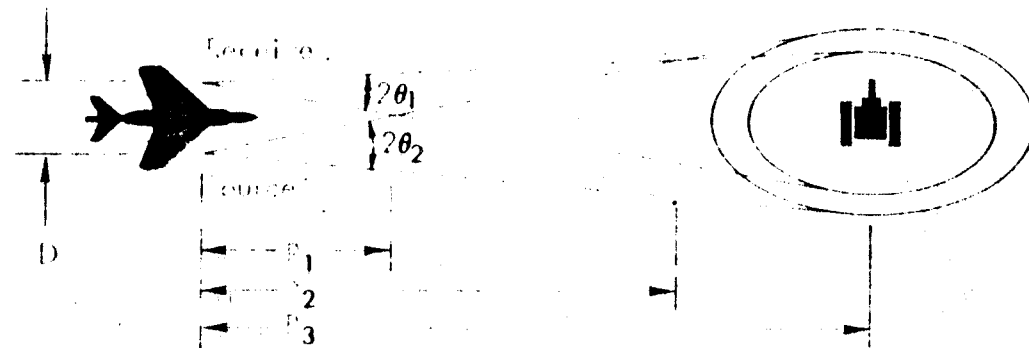
The system outlined in Fig. 1 consists of a monochromatic source of radius Y_2 , emitting a uniform beam of half-angle θ_2 , and a receiver of radius Y_1 , whose field of view half-angle is θ_1 , with $\theta_1 \leq \theta_2$. The range r is measured from the receiver. The centers of source and receiver are separated by a distance D , and the source beam is "squinted" toward the receiver so that the centerlines cross at range R_3 . The angle φ between the centerlines will be referred to as the squint angle.

For ease of exposition, both source beam and receiver field of view will be assumed to have circular cross sections. The modifications necessary for other cross sections are minor, and primarily involve changes in the derivation of the function $f(r)$ described below. The source is assumed to be the only source of illumination; the atmosphere is assumed to be uniform, so that the scattering coefficient, u , and attenuation coefficient, a , are functions of wavelength only. Atmospheric scattering is assumed to be isotropic.

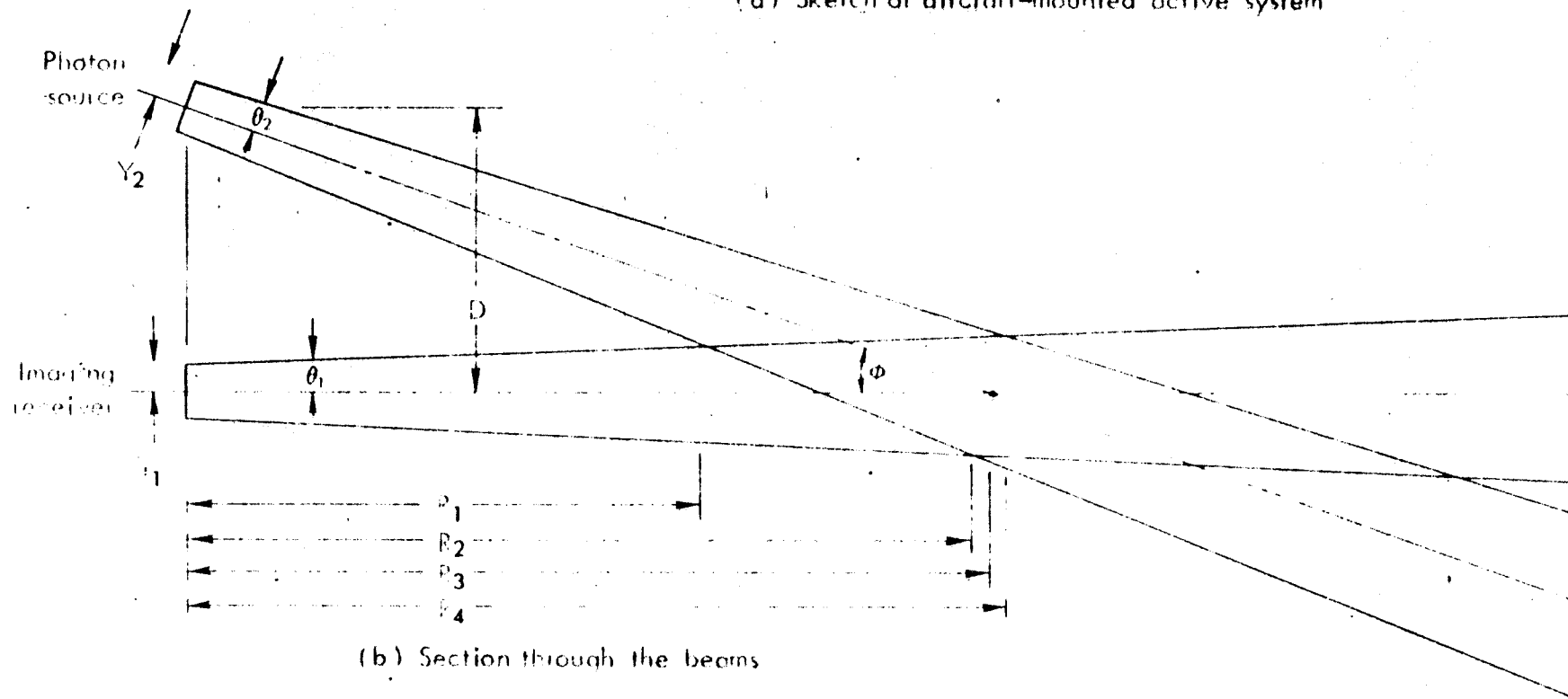
The following ranges*, measured along the receiver centerline, are of interest in describing the performance and the characteristics of the system

$$R_1 = \frac{D - Y_1 - Y_2}{\tan(\theta_1) + \tan(\theta_2 + \varphi)}$$

*These formulas ignore the effect of rotation of the source (through the angle φ) on the source and receiver edge-to-edge distance, which is approximated by $(D - Y_1 - Y_2)$, etc.



(a) Sketch of aircraft-mounted active system



(b) Section through the beams

Fig. 1 - System geometry

$$R_2 = \frac{(D + Y_1 - Y_2)}{\tan(\theta_2 + \varphi) - \tan(\theta_1)}$$

$$R_3 = \frac{D}{\tan \varphi}$$

$$R_4 = \frac{D - Y_1 + Y_2}{[\tan(\theta_1) - \tan(\theta_2 - \varphi)]^+}$$

R_1 is the range at which the receiver field of view first intersects the source beam, R_2 is the range at which the receiver field of view and the source beam completely overlap, R_3 is the range at which the centerlines cross, and R_4 is the range at which the complete overlap of the receiver field of view and the source beam ends.

It is assumed that θ_1 , θ_2 , Y_1 , and Y_2 are such that R_2 is finite and $R_2 \leq R_4$, so that full immersion of the receiver field of view in the source beam does occur. Since $\theta_1 \leq \theta_2$, the finiteness of R_2 requires only that $\varphi > 0$ if $\theta_1 = \theta_2$, and if $\theta_1 < \theta_2$, R_3 may be infinite. The assumption that $R_2 \leq R_4$ requires only that if θ_1 and θ_2 are nearly equal, then Y_1 must be smaller than or nearly equal to Y_2 . The case $R_4 = \infty$ is allowable, and occurs if $\theta_1 \leq \theta_2 - \varphi$. If $r < R_2$, a portion of the area "seen" by the receiver is illuminated by the source; if $R_2 \leq r \leq R_4$ the entire area seen by the receiver is illuminated; if $r > R_4$, a portion of the area seen is illuminated.

If $\varphi > 0$, then the cross section of source beam at

range r (intersection of the cone with a plane at range r from, and parallel to, the plane of the source and receiver) is an ellipse rather than a circle, and the true (slant) range from the centroid of the cross section to the source receiver is slightly greater than r . The derivations which follow neglect this effect and assume that this cross section is a circle at range r from the system. As long as φ is small, the effects of this approximation are minor.

BACKSCATTER

Consider a slice of atmosphere of thickness Δr at range r from the system. Because of attenuation, the beam flux is e^{-ar} of the flux emitted by the source. A portion $u\Delta r$ is scattered within the slice, and some fraction $f(r)$ of this is within the receiver field of view. If r is sufficiently large relative to Y_1 , then approximately $Y_1^2/4r^2$ of the scattered energy is directed toward the receiver, and this energy is again attenuated by a factor of e^{-ar} . Thus, considering only first-order backscatter effects*, the fraction of emitted energy seen by the receiver as backscatter from the slice of atmosphere under consideration is approximately

$$\Delta B(r) = \frac{Y_1^2 f(r) u e^{-2ar}}{4r^2} \Delta r \quad (1)$$

Since the fraction of the source beam cross section seen by the receiver, $f(r)$, is zero for $r < R_1$, Eq. (1) is a

*As long as the path under consideration is not characterized by extremely high attenuation (i.e. is not through a dense fog) multiple scattering effects can be neglected.

good approximation for all values of r provided that R_1 is large relative to Y_1 . Taking limits in the usual manner, it is then found that the fraction of emitted energy seen by the receiver as backscatter from ranges less than or equal to r is approximately.

$$B(r) = \int_0^r \frac{Y_1^2}{4s^2} f(s) u e^{-2as} ds \quad (2)$$

Similarly, the fraction of the emitted energy reflected from a Lambertian target of reflectivity 1.0 occupying the entire field of view of the receiver is

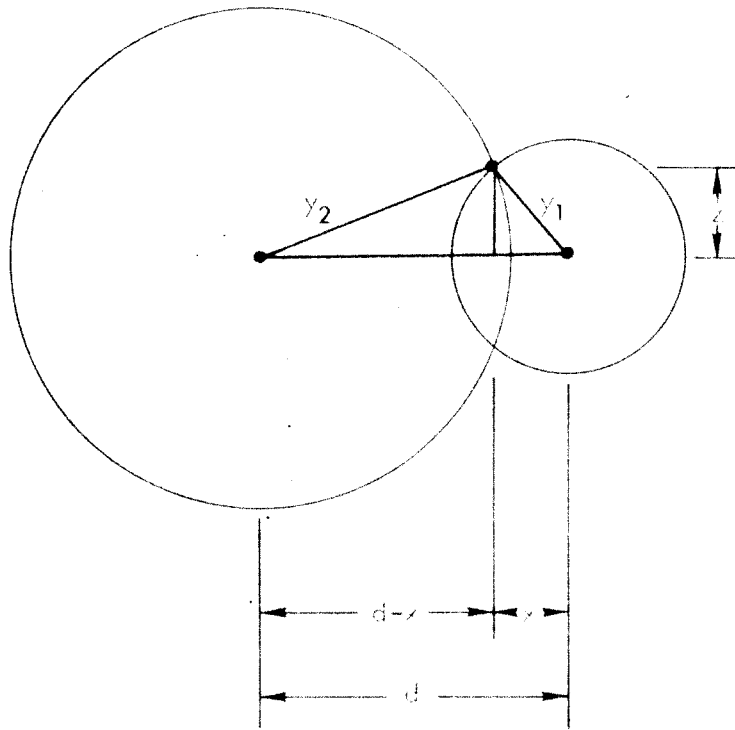
$$S(r) = \frac{Y_1^2}{r^2} f(r) e^{-2ar} \quad (3)$$

DERIVATION OF f

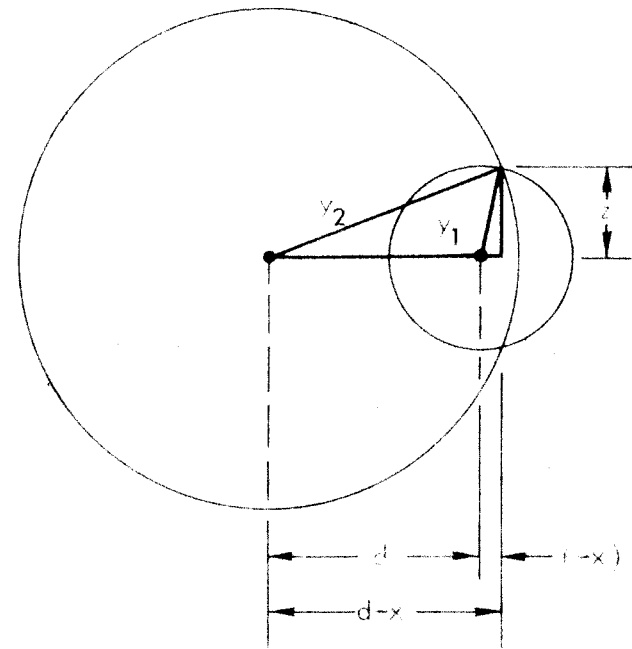
At a range r from the receiver, the source beam and receiver field of view centerline are separated by a distance $d(r) = D - r \tan \varphi$, and the receiver field of view cross section is a circle of radius $y_1(r) = Y_1 + r \tan \theta_1$. For φ small, the source beam cross section can be approximated by a circle of radius $y_2(r) = Y_2 + r \tan \theta_2$.

The receiver field of view begins to intercept the source beam at range R_1 ; it is completely immersed in the source beam at range R_2 . For ranges between R_1 and R_2 , the cross section will appear as shown in Fig. 2a or 2b.

Let $x(r)$ be the distance from the chord joining the intersections of the circumferences of the two circles to



(2a) When $y_2^2 < y_1^2 + d^2$



(2b) When $y_2^2 > y_1^2 + d^2$

Fig. 2—Sectional view through the illuminating source beam and receiver beam

the receiver field of view centerline, measured in a direction away from the source beam centerline (thus $x < 0$ in Fig. 2b), and let $z(r)$ be half the length of the chord. Then

$$x = \frac{y_1^2 + d^2 - y_2^2}{2d}$$

$$z = \sqrt{y_1^2 - x^2} = \sqrt{y_2^2 - (d - x)^2}$$

where the functional dependence on r is suppressed. The area of the intersection of the two circles is given by

$$\begin{aligned} & (y_1^2 \tan^{-1}\left(\frac{z}{x}\right) - zx) + (y_2^2 \tan^{-1}\left(\frac{z}{d-x}\right) - z(d-x)) \\ &= y_1^2 \tan^{-1}\left(\frac{z}{x}\right) + y_2^2 \tan^{-1}\left(\frac{z}{d-x}\right) - zd \end{aligned}$$

where $0 \leq \tan^{-1}\left(\frac{z}{x}\right) < \pi$. Since the area of the source beam circle is πy_2^2 , the fraction of the source beam seen by the receiver at range r is given by

$$\begin{aligned} f(r) &= 0, & : r \leq R_1' \\ &= \frac{1}{\pi} \left(\frac{y_1^2}{y_2^2} \tan^{-1}\left(\frac{z}{x}\right) + \tan^{-1}\left(\frac{z}{d-x}\right) - \frac{zd}{y_2^2} \right); & R_1' < r < R_2' \quad (4) \\ &= y_1^2/y_2^2, & : R_2' \leq r < R_4 \end{aligned}$$

where the functional dependence on r is again suppressed and R_1' and R_2' are the approximations to R_1 and R_2 given

below. These result from the approximating assumption that the source beam cross section at range r is circular, rather than elliptical.

$$R_1' = \frac{D - Y_1 - Y_2}{\tan(\theta_1) + \tan(\theta_2) + \tan(\varphi)}$$

$$R_2' = \frac{D + Y_1 - Y_2}{\tan(\theta_2) + \tan(\varphi) - \tan(\theta_1)}$$

GATED SYSTEMS

One method of reducing the backscatter which reaches the receiver is gating. A gated system is one in which the source and receiver are operated in a cyclic, rather than continuous, manner. The source is pulsed on during the first part of the cycle, at which time the receiver is turned off. The receiver is turned on at some time later in the cycle, and thus receives less backscatter. If $g(r)$ is the fraction of the return which the receiver accepts from range r , then Eq. (2) becomes

$$B(r) = \int_0^r \frac{Y_1^2}{4s^2} f(s)g(s)ue^{-2as} ds \quad (5)$$

and Eq. (3) becomes

$$S(r) = \frac{Y_1^2}{r^2} f(r)g(r)e^{-2ar} \quad (6)$$

If it is assumed that the source and receiver have zero rise and fall times, i.e., the source pulse is a rectangular wave and the receiver turns on and off instantly, the gating characteristics of the system are determined by the various times needed to describe a single cycle:

T_0 = time source is turned on at the beginning of the cycle.

T_1 = time source is turned off.

T_2 = time receiver is turned on.

T_3 = time receiver is turned off ($T_3 > T_2$).

T_4 = time source is turned on again at the beginning of the next cycle ($T_4 > T_3$).

The return from range r begins to reach the receiver at time $T_0 + 2r/c$, where c is the velocity of light. The receiver is not turned on until time T_2 , hence the receiver begins to see return from range r at time $\max(T_0 + 2r/c, T_2)$. The receiver turns off at time T_3 , and the last of the return from range r reaches the receiver at time $T_1 + 2r/c$, hence the receiver ceases to see return from range r at time $\min(T_3, T_1 + 2r/c)$. The total length of the pulse is $T_1 - T_0$, hence

$$g(r) = \frac{[\min(T_3, T_1 + 2r/c) - \max(T_0 + 2r/c, T_2)]^+}{T_1 - T_0} \quad (7)$$

for $r < (T_4 + T_2 - T_1 - T_0)c/2$, the range at which the receiver begins to accept return from the previous pulse.

The graph of g for fixed values of T_2 and T_3 and

several values of T_1 is shown in Fig. 3.

The more general situation, when the source pulse is not a square wave and the receiver does not turn on and off instantly, is similar, though somewhat more complex conceptually. Let $h_1(t)$, $0 \leq h_1 \leq 1$, be the fraction of impinging energy being accepted by the receiver at time t . (During the receiver turn-on or turn-off transient, $h_1 < 1$; when the receiver is in the steady-state $h = 1$, or $h = 0$.) Let $h_2(t)$ be the fraction of average source power being emitted at time t . (Note that $h_2(t)$ will be greater than one for some values of t , and that $(\frac{1}{T_4 - T_0}) \int_{T_0}^{T_4} h_2(t) dt = 1$.) Then

$$g(r) = \frac{1}{T_4 - T_0} \int_{T_0}^{T_4} h_1(t) h_2(t - 2r/c) dt \quad (8)$$

In the case discussed above (zero receiver and source rise and fall times), $h_2(t) = (T_4 - T_0)/(T_1 - T_0)$ if $T_0 \leq t \leq T_1$, $h_2(t) = 0$ otherwise; and $h_1(t) = 1$ if $T_2 \leq t \leq T_3$, $h_1(t) = 0$ otherwise. For these functions, h_1 and h_2 , Eqs. (7) and (8) are equivalent.

The effect of gating, then, is to produce a range "window" which is seen by the receiver. Any energy returned to the receiver from outside the window will not be seen, whether the return is backscatter or target return. In general, Eq. (8) gives the size and shape of the range window. In the particular case where rise and fall times are negligible, Eq. (8) reduces to Eq. (7), and the shape

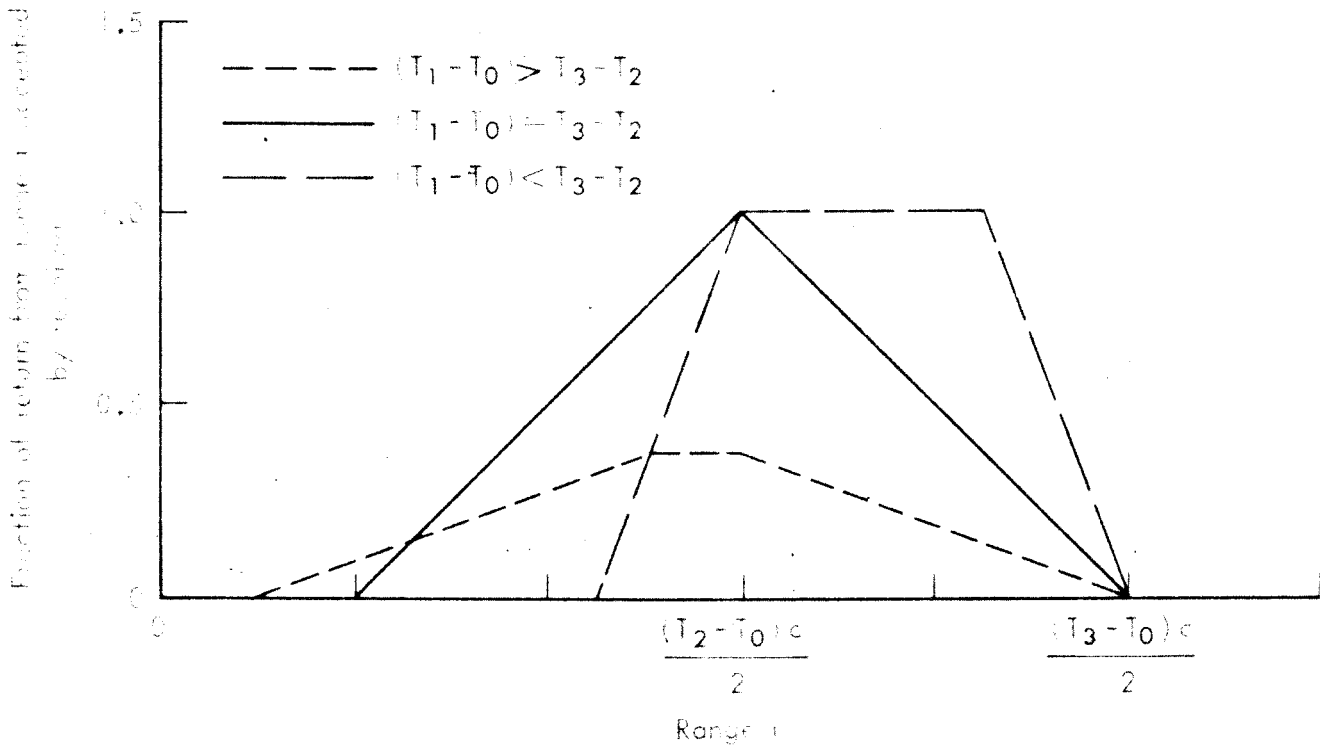


Fig. 3—The function $g(r)$

of the window is as shown in Fig. 3. If the source pulse length is the same as the receiver on time ($T_1 - T_0 = T_3 - T_2$), the window is triangular, with height 1, upper vertex at $(T_2 - T_0)c/2$, and lower vertices at $(T_2 - T_1)c/2$ and $(T_3 - T_0)c/2$.

If source pulse and receiver on-time are unequal, the window is trapezoidal, with the same lower vertices and with upper vertices at $(T_3 - T_1)c/2$ and $(T_2 - T_0)c/2$. If the source pulse is shorter ($T_1 - T_0 < T_3 - T_2$), the height of the window is 1; while if the source pulse is longer ($T_1 - T_0 > T_3 - T_2$), the height of the window is $(T_3 - T_2)/(T_1 - T_0)$; i.e., there is no range from which the receiver accepts the full energy returned.

In order to allow full use of the source power, the source pulse must be shorter than the receiver on time. Moreover, for a fixed receiver on time and average power, the window can be made "sharper" by decreasing the pulse length. A system with a "sharp" range-window will be limited in range, for it will only see targets which fall within the window, but the backscatter from ranges outside the window will be eliminated.

EVALUATION OF PERFORMANCE

In order to evaluate system performance, some assumptions concerning the nature of the target detection problems are required. The problem is assumed to be that of detecting a small target area of uniform reflectivity ρ_1 against a

background of known reflectivity ρ_0 , and the signal-to-noise ratio (defined below) is assumed to provide a measure of the system's ability to perform this task. Because of the nature of the statistical decision problem involved, the signal-to-noise ratio does not, in itself, provide a precise measure of system performance (for reasons which are outlined below). It has the advantage, however, of being a simple measure in common use, and this, coupled with the lack of any better alternative, favors its adoption. The discussion which follows neglects the fact that the backscatter is not uniform across the receiver field of view, but is stronger in the portion of the field nearest the source and weaker in the portion of the field away from the source (see Fig. 1). The signal-to-noise ratio derived below (Eq. (13)) therefore represents the expected signal-to-noise ratio resulting from random placement of the target within the receiver field of view.

The visual detection problem in the case of monochromatic radiation may be reduced to photon counting. The source emits an average power of W watts, or an average photon flux of kW photons/sec, where k is the number of photons per joule produced by the source radiation. The average number of photons seen by the receiver during an observation interval of τ seconds as reflected from a square target of side l and reflectivity ρ_1 at range r is therefore

$$\lambda_1 = \frac{\ell^2}{\pi y_1^2(r)} q k \tau W (\rho_1 S(r) + B(r)) \quad (9)$$

where q is the overall quantum efficiency (probability a photon entering the receiver aperture will be counted) of the receiver and $y_1(r)$ is the radius of the receiver field of view at range r . If the target is assumed to be against a uniform background of reflectivity ρ_0 , then, in the absence of a target, an average number

$$\lambda_0 = \frac{\ell^2}{\pi y_1^2(r)} q k \tau W (\rho_0 S(r) + B(r)) \quad (10)$$

would be expected. The signal from the target (difference between expected flux with and without a target present) is therefore

$$S = \lambda_1 - \lambda_0 = \frac{\ell^2 q k \tau W}{\pi y_1^2(r)} (\rho_1 - \rho_0) S(r) \quad (11)$$

The number of photons received is random, with a distribution which can be approximated as Poisson with mean λ_1 if a target is present and λ_0 if no target is present. The standard deviation of the Poisson distribution is the square root of its mean; therefore, the standard deviation in the number of photons seen if no target is present (noise) is

$$N = \sqrt{\lambda_0} = \left(\frac{\ell^2}{\pi y_1^2(r)} q k \tau W (\rho_0 S(r) + B(r)) \right)^{\frac{1}{2}} \quad (12)$$

The signal-to-noise ratio is thus

$$\frac{S}{N} = \frac{\lambda_1 - \lambda_0}{\sqrt{\lambda_0}} = \frac{t}{y_1(r)} \sqrt{\frac{qk\tau W}{\pi}} \frac{(\rho_1 - \rho_0)S(r)}{(\rho_0 S(r) + B(r))^{\frac{1}{2}}} \quad (13)$$

The noise, as defined by Eq. (12), reflects the variation which would occur in the number of photons received if no target were present. Because of the Poisson nature of the process, this variation is different from that which would occur in the presence of a target. It is for this reason that the signal-to-noise ratio is not, by itself, a precise indicator of system performance. While a detailed analysis of this question is beyond the scope of this Memorandum, a few remarks concerning the difficulties involved are in order. A further discussion of the statistical concepts used can be found in any standard text on statistics, such as Mood (1).

The statistical decision problem involved is that of testing the hypothesis that no signal is present. The performance of any test of that hypothesis may be described in terms of the level of significance of the test or probability that a target is detected when none is present, and the power of the test or the probability that a true target is detected. The power of the test depends, of course, on the particular alternative (target reflectivity) in question. The simplest case is that where both the background reflectivity ρ_0 and target reflectivity ρ_1 are constant and known. Without loss of generality, assume $\rho_0 < \rho_1$. The most

powerful test, at a given level of significance, decides a target is present if and only if the observed number of photons exceeds some threshold, λ , and the threshold chosen reflects a tradeoff between false-alarm probability and detection probability. The false-alarm probability can be decreased only by accepting a decrease in the probability of detection of a true target. Unless λ_0 is small, i.e., less than 5, the distribution of the observed number of photons when no target is present is approximately normal with mean λ_0 and standard deviation $\sqrt{\lambda_0}$. The level of significance of the test is thus a function only of the threshold signal-to-noise ratio, $(\lambda - \lambda_0)/\sqrt{\lambda_0}$. (It is this threshold signal-to-noise ratio which is discussed by Rose⁽²⁾.) The distribution of the observed number of photons under the alternative (target present), however, is approximately normal with mean λ_1 and standard deviation $\sqrt{\lambda_1}$, and the power of the test is a function of both the signal-to-noise ratio (Eq. (13)) and of λ_1 (or alternatively, of the signal-to-noise ratio and λ_0). Without knowledge of the actual value of either λ_1 or λ_0 , the only general statement which can be made is that the power of the test is a strictly increasing function of λ_1 and is equal to .5 for $\lambda_1 = \lambda$.

This difficulty cannot be resolved by any alternative definition of noise. If $\sqrt{\lambda_1}$ is used, for example, instead of $\sqrt{\lambda_0}$, the power of the test will be a function of the signal-to-noise ratio only, but the level of significance

will not. Moreover, there appears to be further justification for the use of $\sqrt{\lambda_0}$. In many practical situations, background reflectivity can be accurately estimated, either because the background can be observed over a long time period, or because the background occupies a much larger fraction of the scene viewed, or both. Furthermore, targets would be expected to occur only infrequently in terms of observation time, or relative area, or both. This latter assumption would tend to dictate a test designed to achieve a fixed false alarm probability, or level of significance, with the resulting determination of the power, or detection probability, against various target alternatives. It is in this context that Rose's discussion of threshold contrast ⁽²⁾ has meaning. Since the level of significance of the test is determined by the threshold signal-to-noise ratio, $(\lambda - \lambda_0)/\sqrt{\lambda_0}$, these assumptions would favor the use of $\sqrt{\lambda_0}$ as noise in defining a signal-to-noise ratio.

The power of the test for a fixed signal-to-noise ratio (Eq. (13)), as a function of λ_0 , flattens out and approaches a constant as λ_0 increases, so the precision with which the signal-to-noise ratio describes the overall performance of the system (the tradeoff between level of significance and power of the test) increases with λ_0 .

The detection model described herein considers only the photoelectrons available to the system, and assumes that the information available from these photoelectrons

is used in an optimal manner to decide whether a target is present or absent. In this sense, the model describes ideal, rather than actual, performance. Factors not considered here, such as additional amplification stages, display electronics, and human factors such as the operator's proficiency, fatigue, etc., would only degrade, and never enhance, system performance.

There are, of course other difficulties in the use of this model for evaluation of actual systems. The target detection problem described in this section is an extremely simplified one. Target scenes of interest in the real world seldom consist of a uniform target against a uniform background. The difficulties involved in adequately defining and describing a typical target scene and in modeling the detection and identification problem given such a description, however, preclude a more realistic model.

Further, no consideration has been given to the fluctuations in the attenuation coefficient which would occur in a real, nonhomogeneous atmosphere; such atmospheric inhomogeneities would appear as additional fluctuations in the photon count received.

III. EFFECTS OF SYSTEM PARAMETERS ON SIGNAL-TO-NOISE RATIO

Insofar as signal-to-noise ratio (Eq. (13)) is a valid measure of system performance, it is possible to draw conclusions regarding the effects of various system parameters on that performance. Some effects, such as those relating to changes in target area, are clear; others, such as the effects of radiated wavelengths, are not.

The signal-to-noise ratio may be separated into two factors. The first, $(\iota/y_1(r))\sqrt{qk\tau W/\pi}$, contains the effects of source power, target size, and receiver efficiency. This is easiest to analyze. S/N can be seen to depend linearly on the square root of those factors which have a linear effect on the number of photons received, such as power (W), receiver efficiency (q) and target area (ι^2). Alternatively, $\iota^2/\pi y_1^2(r)$, the fraction of the receiver field of view filled by the target, can be considered.

Consider the second factor in the signal-to-noise ratio, $(\rho_1 - \rho_0)S(r)/(\rho_0 S(r) + B(r))^{\frac{1}{2}}$. This contains the effects of scattering, attenuation, and target and background reflectivities. The reflectivities ρ_1 and ρ_0 are physical characteristics of the target and background and may depend on the wavelength of the illumination. $S(r)$ depends on the wavelength of the illumination, atmospheric conditions affecting attenuation, range, and the size of the receiver aperture. These factors themselves set an

upper limit on achievable system performance.

Actual performance is degraded from this upper limit because of the backscatter factor $B(r)$, which depends on the geometry of the system and the gating in addition to those factors which influence $S(r)$. The amount of energy which is scattered by the atmosphere is greatest near the source, and drops off rapidly as range increases. It is highly desirable, therefore, that the receiver not see this near backscatter. In ungated systems, the amount of backscatter seen by the receiver at range r is proportional to $f(r)$. (See Eq. (1).) No backscatter is seen at ranges $r < R_1$, hence it is desirable that R_1 be made as large as possible, consistent with other constraints on the system. Other factors being equal, R_1 increases with D , the separation between source and receiver, so that increased separation decreases received backscatter. However, there are practical limitations on the separation which can be obtained, particularly with vehicular systems. Narrow field of view systems receive less backscatter than do systems with a wider field of view, but at the cost of decreasing the area seen. The most promising method of decreasing backscatter without adversely affecting the system in other ways is gating, although this makes the system more complex, as well as adding constraints on performance.

The signal-to-noise ratio imposes limitations on the size target which can be detected with any given degree of reliability. More stringent limitations, however, are placed

on the size target which can be recognized and identified. To identify a tank, plane, or man as such requires more than the ability to detect a target of that size. It requires the ability to detect much smaller targets to be able to discern the outline of the larger target. A man, for example, represents a target whose area is about a square meter. Identification of a man as such, however, may require reliable detection capability for targets of the order of 0.01 m^2 , so that the general shape of the man can be seen.

The system's angular resolution may, of course, also be limited by purely geometric considerations; for instance, any system in which the human eye is the final imaging surface must have adequate resolution so that adjacent points are imaged onto different sensory elements in the retina. Similarly, if photographic film is used for imaging, the film's resolution characteristics must be compatible with the resolution desired. This limitation is not considered in the present formulation.

IV. ILLUSTRATIVE SYSTEMS

To illustrate the application of these ideas, three hypothetical systems have been evaluated using the JOSS* computer system, and the results presented in Figs. 6 through 23 and Table 3. In order to limit the number of parameter combinations considered, all parameters not directly affecting the backscatter calculation have been fixed at a single value throughout these calculations. Signal-to-noise ratios for other values of these parameters can be obtained from those shown by a simple linear transformation of the signal-to-noise scale. Table 1 lists the values used and the reasons for their choice.

Table 2 lists the parameters which define each system. The systems differ primarily in the source beam and receiver field of view angles. Systems with receiver fields of view of 20° , 7° , and 2° are labeled general-purpose, intermediate, and narrow-angle system, respectively. Each system has been evaluated for three values of visibility, 5, 20 and 50 km, corresponding to fair, good, and excellent visibility, and for three source wavelengths, 400, 600, and 800 nm, corresponding to near-ultraviolet (UV), visible, and near-infrared (IR) radiation, respectively. A source-receiver separation of 1 m is used for the 5 and 20-km visibility computations and a separation of 10 m used for the 50-km visibility computation. These curves may therefore be considered lower

*JOSS is the trademark and service mark of The RAND Corporation for its computer program and services using that program.

Table 1

PARAMETERS WHICH ARE COMMON TO ALL SYSTEMS

Parameter	Value	Reason for Consideration
Source power	100 W	Considered attainable in an airborne system.
Target reflectivity	.2	Typical of military targets, e.g., tanks, personnel, etc., reflectivity usually higher in visible and IR than in UV.
Background reflectivity	.1	Typical of much outdoor terrain.
Observation interval	.2 sec	Typical of light-adapted human eye viewing a bright display.
Target size	1 m ²	Resolution required to detect trucks and other military targets.

Table 2

PARAMETERS OF SPECIFIC SYSTEMS

Type of System	Receiver Half-angle (deg)	Source Half-angle (deg)	Receiver Diameter (in.)	Source Diameter (in.)
General purpose	10.0	12.5	5	22
Intermediate	3.5	5.0	5	22
Narrow angle	1	1.5	5	12

and upper bounds for all cases where $1 \leq D \leq 10$ and $5 \leq V \leq 50$.

Figure 4 is a plot of quantum efficiency of the S-20 phosphor.⁽³⁾ The shape of the S-20 curve in the region above 700 nm is not clearly defined--it is shown as a dashed line in Fig. 4. The values used in the JOSS program are taken from the S-20 curve shown. A nominal optical transmission of 0.9 is assumed for the rest of the optical system, regardless of wavelength. Thus the value of q used in Eq. (13) is equal to 0.9 times the appropriate value read from Fig. 4.

The scattering coefficient per meter is given by

$$u = \frac{3.91 \times 10^{-3}}{V} \left(\frac{550}{\lambda} \right)^{0.585} V^{\frac{1}{3}}$$

where V is the visibility in km and λ is the wavelength in nanometers (nm). This formula, derived in Ref. 4, is valid in and near the optical region of interest here, 300 to 1000 nm. Figure 5 is a graph of the values of u as a function of V , obtained from use of this formula, for $\lambda = 400, 600,$ and 800 nm.

The attenuation coefficient, a , equals scattering plus absorption. However, atmospheric absorption is sufficiently small in the 300 to 1000 nm region that it is neglected here, i.e., a is taken to be equal to u .

It is assumed that each system's source is "squinted"

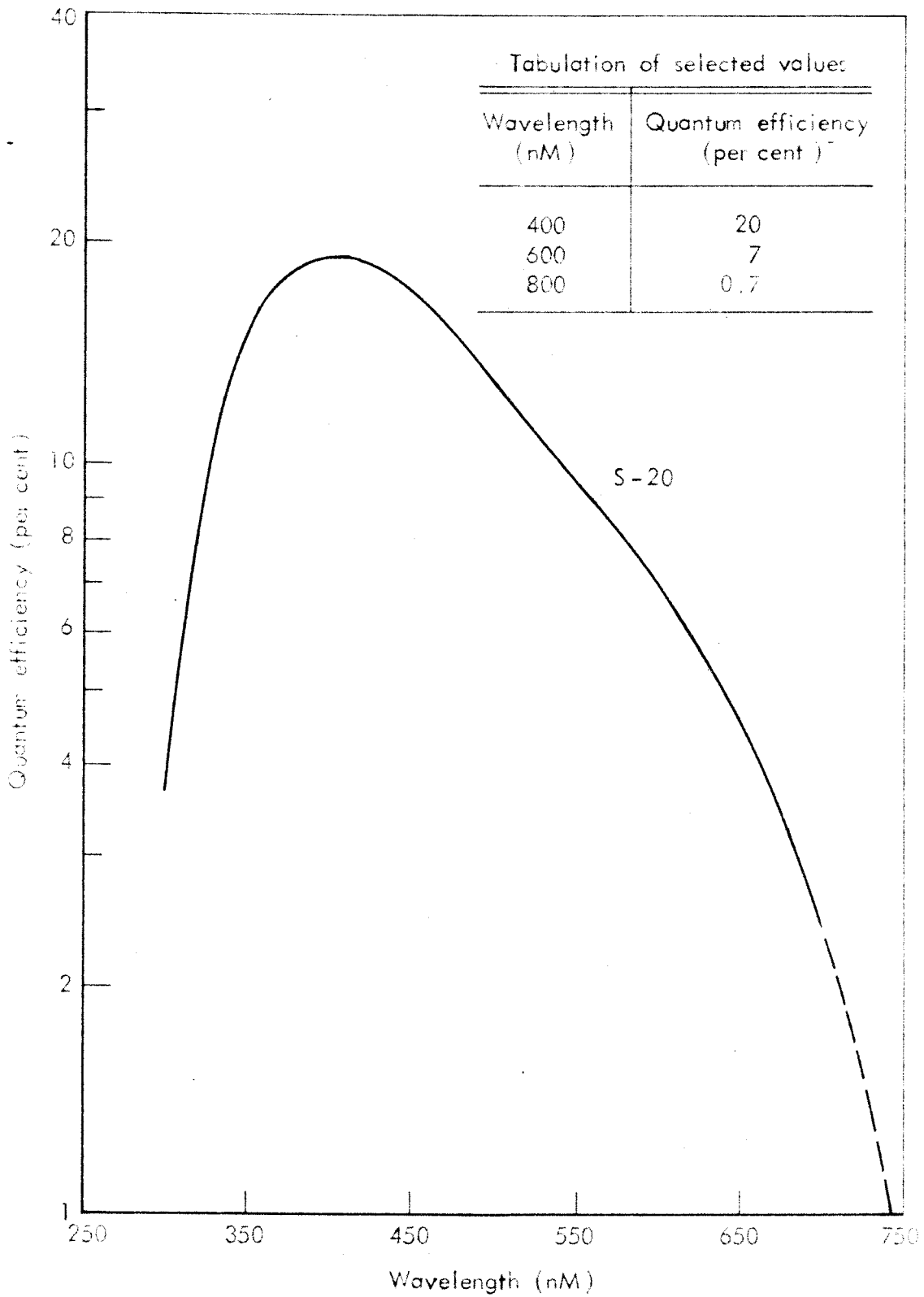


Fig. 4—Quantum efficiency of S-20 phosphors

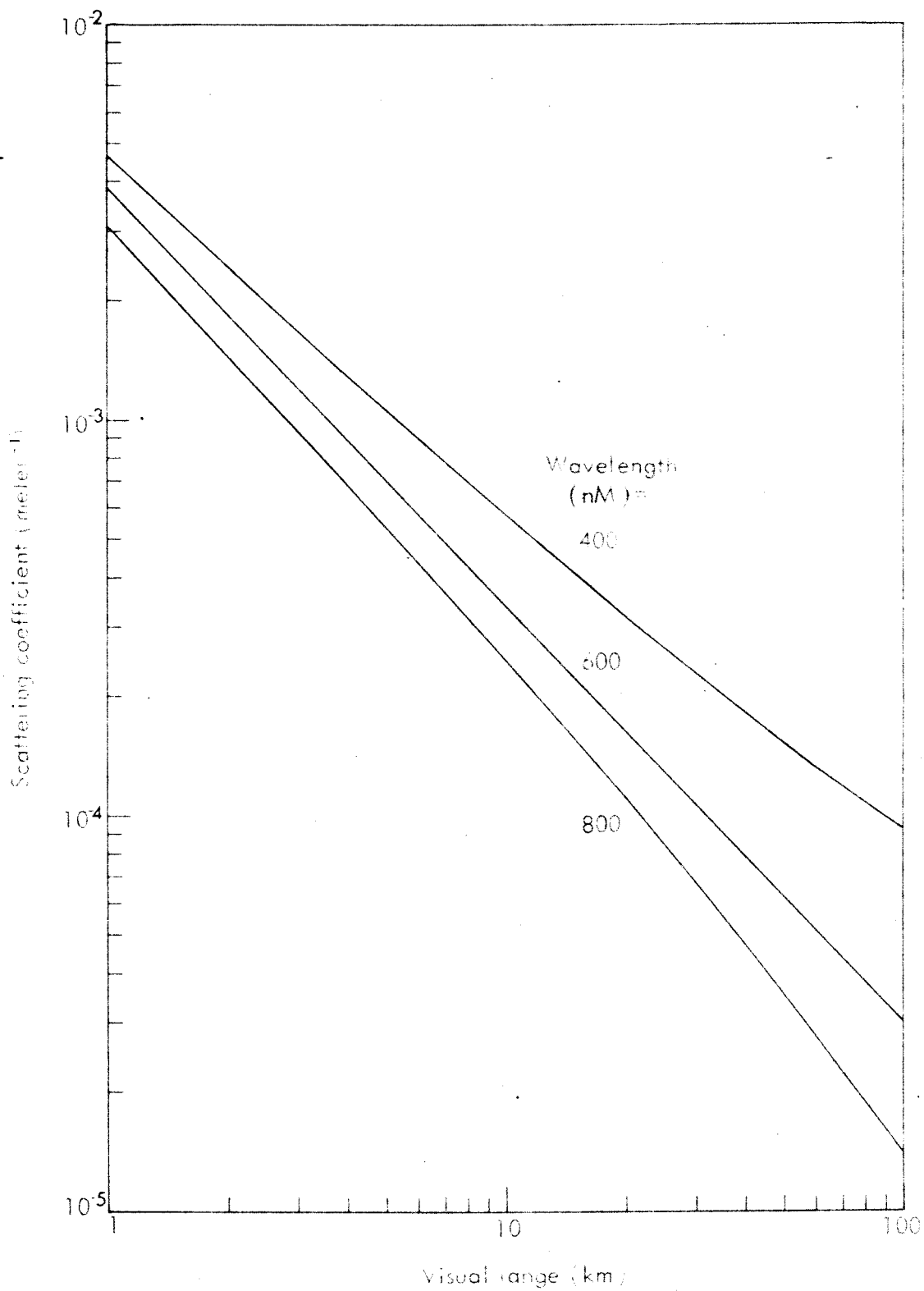


Fig.5—Scattering coefficient as a function of visual range

so the beam centerlines cross at 1000 m, and that a uniform target appears against a uniform background at all ranges from where the receiver beam is initially immersed in the source beam (R_2) to 5000 m. The target element is of the same size, regardless of range.

V. COMPUTATIONAL RESULTS AND CONCLUSIONS

Figures 6 through 14 each contain signal-to-noise plots for the systems evaluated. A high value of signal-to-noise ratio does not mean that the system analyzed would necessarily perform well in the stated environment, but a low value does mean that it would not perform well. The division between a high and low value of signal-to-noise ratio occurs somewhere between 10 and 3.

Figures 15 through 23 are graphs of the output power which would be required of the three aforementioned systems to achieve a signal-to-noise ratio of 10 at specified ranges.

Rather than choose representative timing values for gated systems, an upper bound on the performance of all gated systems has been computed. Each graph includes plots labeled "perfect gating" for each visibility; this is the signal-to-noise ratio which would be achieved by the elimination of all backscatter. It could be achieved in a gated system only if all the radiant energy were delivered in a pulse of negligible duration and all backscatter were gated out. The "perfect gating" values are not the same as those which would be achieved by a system operating in a vacuum; the unavoidable two-way atmospheric attenuation is included in the "perfect gating" calculations. Thus, the "perfect gating" plot establishes an upper bound for the performance of any system operating within an

attenuating atmosphere.

Portions of Figs. 6 through 14 are summarized in Table 3, which shows the ranges corresponding to the signal-to-noise ratios of 3 and 10 on each of the graphs. Insofar as signal-to-noise ratio is an adequate measure of system performance, this band provides lower and upper bounds on the maximum useful range of the systems evaluated.

Under comparable conditions, the range of the narrow-angle system is greatest, and that of the general-purpose system is least. This is due to two factors:

1. The smaller source beam and receiver field of view result in an increase in R_1 , the range at which the source beam and receiver field of view intersect.

2. The fixed source power concentrated in a narrower beam results in higher power density on the target. This increase is achieved at the cost of a decrease in area viewed, however, and this decrease in viewing area may limit the utility of narrow-angle systems.

Using the given parameters, the system operating at 600 nm has greater detection range than either the UV (400 nm) or IR (800 nm) system. However, the results are heavily biased against the near IR system because of the low quantum efficiency (0.7%) used for the S-20 surface at 800 nm. If a more efficient phosphor for the near IR were available, the performance of near IR systems would be competitive with, or superior to, that of systems

Table 3

RANGES (meters) CORRESPONDING TO SIGNAL-TO-NOISE RATIOS BETWEEN 10 AND 3
FOR SYSTEMS WITH 100 WATTS OUTPUT POWER

System	Receiver Half Angular Field, Degrees	Gating	$\lambda = 400$		$\lambda = 600$		$\lambda = 800$	
			D = 1 V = 5	D = 10 V = 50	D = 1 V = 5	D = 10 V = 50	D = 1 V = 5	D = 10 V = 50
General-Purpose	10	None	600-750	1450-2050	600-800	1600-2350	500-700	1300-1950
		Perfect	1600-2100	2950-4700	1750-2450	2900-4900	1300-2000	1900-3200
Inter-mediate	3.5	None	750-950	2150-2950	850-1100	2450-3550	700-1000	2000-3200
		Perfect	1950-2500	4250-5000 ⁺	2200-3000	4350-5000 ⁺	1800-2600	2850-5000
Narrow-Angle	1	None	1100-1350	3400-4550	1250-1600	4150-5000 ⁺	1100-1500	3400-5000
		Perfect	2600-3300	5000+	3000-3900	5000+	2650-3700	5000+

λ = wavelength, nm.

D = separation between source and receiver, m.

V = visibility, km.

operating in the visible. Even with the performance penalty imposed, it can be seen that the performance of the near IR system is very similar to that of the UV system. Furthermore, important wavelength-dependent parameters have been treated as wavelength-invariant in these calculations; both material reflectivities and lamp output power are functions of wavelength. Considering these factors as such might alter the comparative detection ranges of one wavelength region vis-à-vis another.

As can be seen from Figs. 6 through 23, the detection ranges achieved by ungated systems and by gated systems are significantly different and indicate the increase in range to be expected through the use of gating or other techniques which reduce backscatter. The limitations placed on ungated systems by backscatter may, in fact, preclude their use in airborne applications where range is of paramount importance.

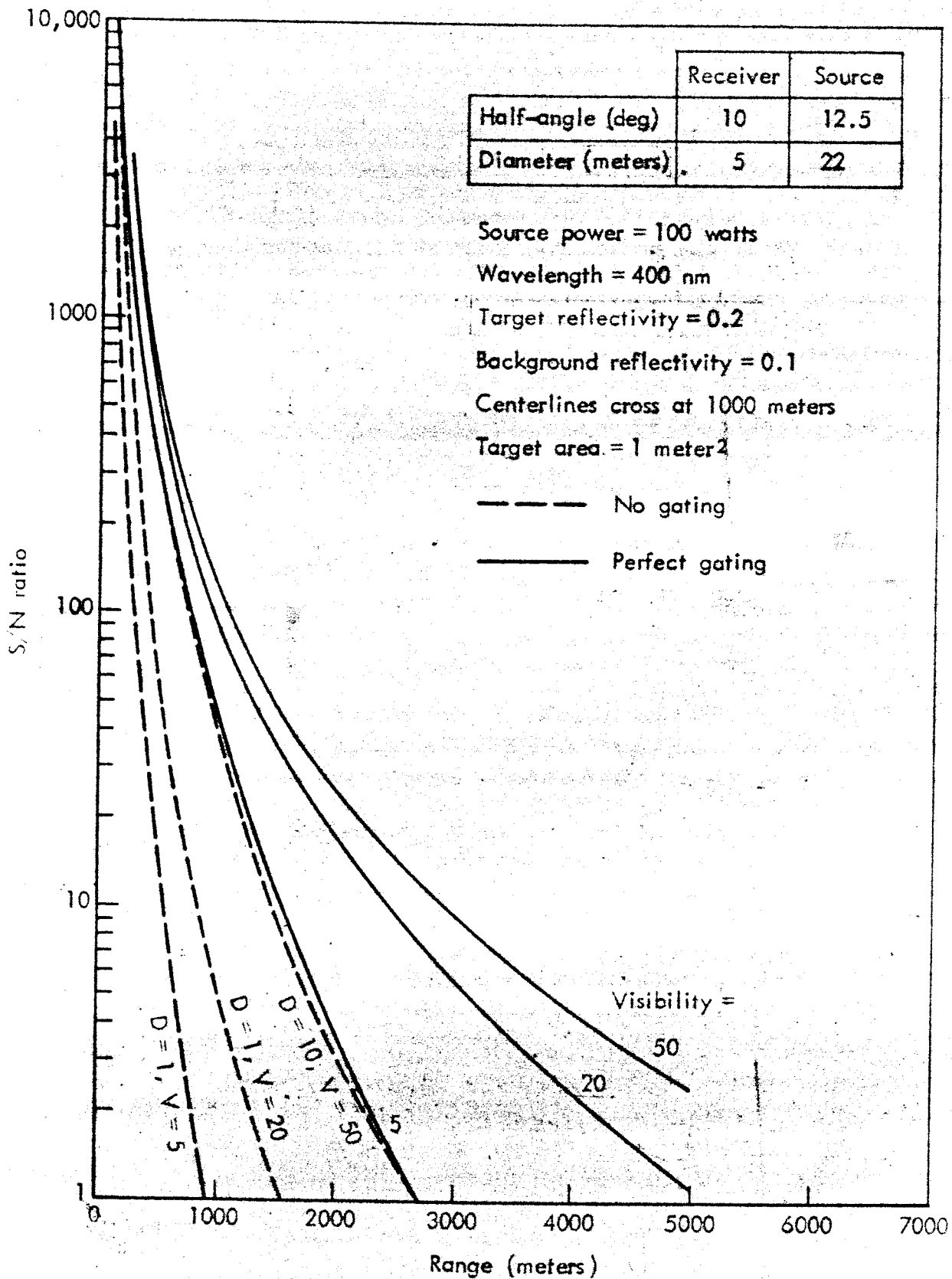


Fig. 6— S/N characteristics of General Purpose System ($\lambda = 400 \text{ nm}$)

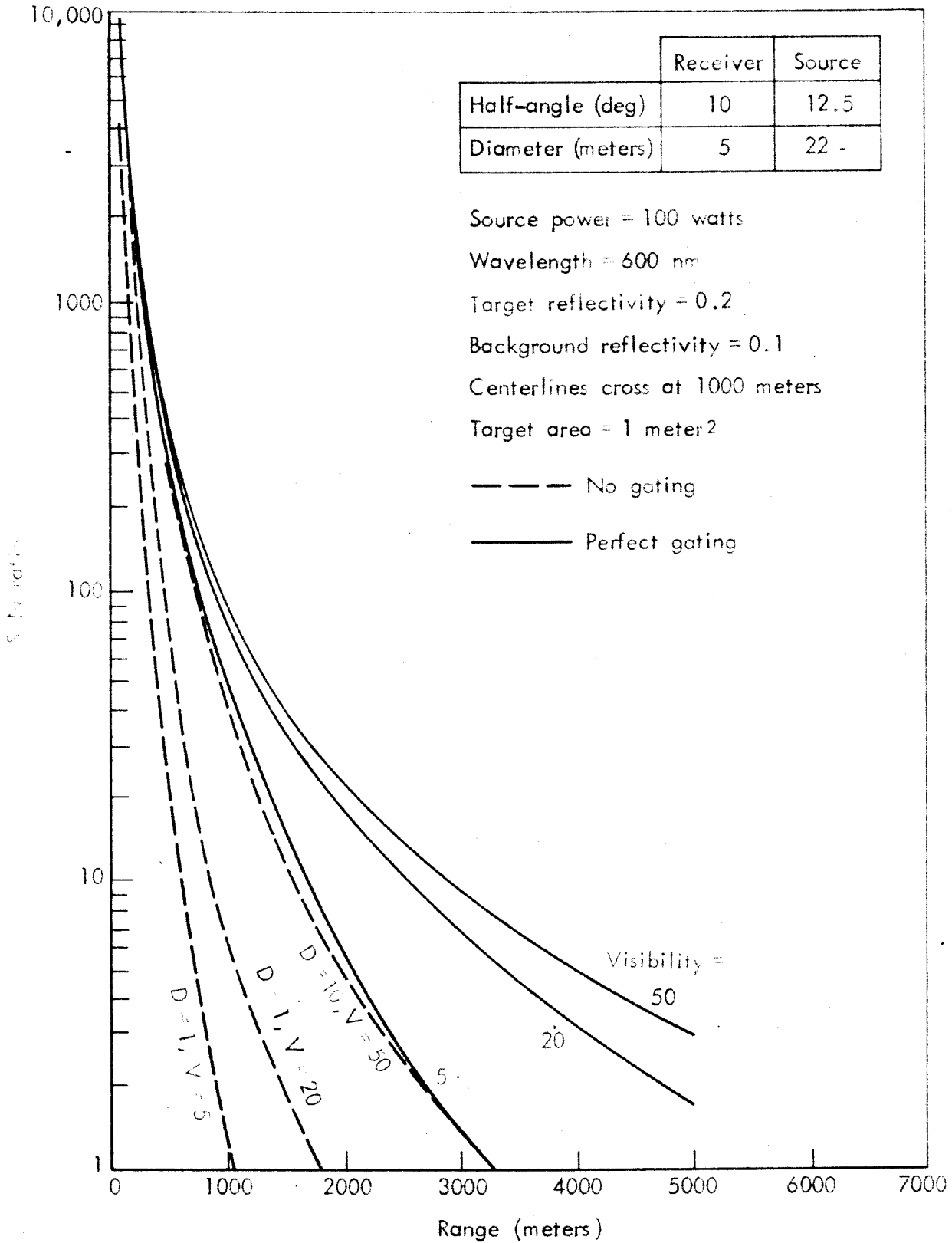


Fig. 7—S/N characteristics of General Purpose System ($\lambda = 600 \text{ nm}$)

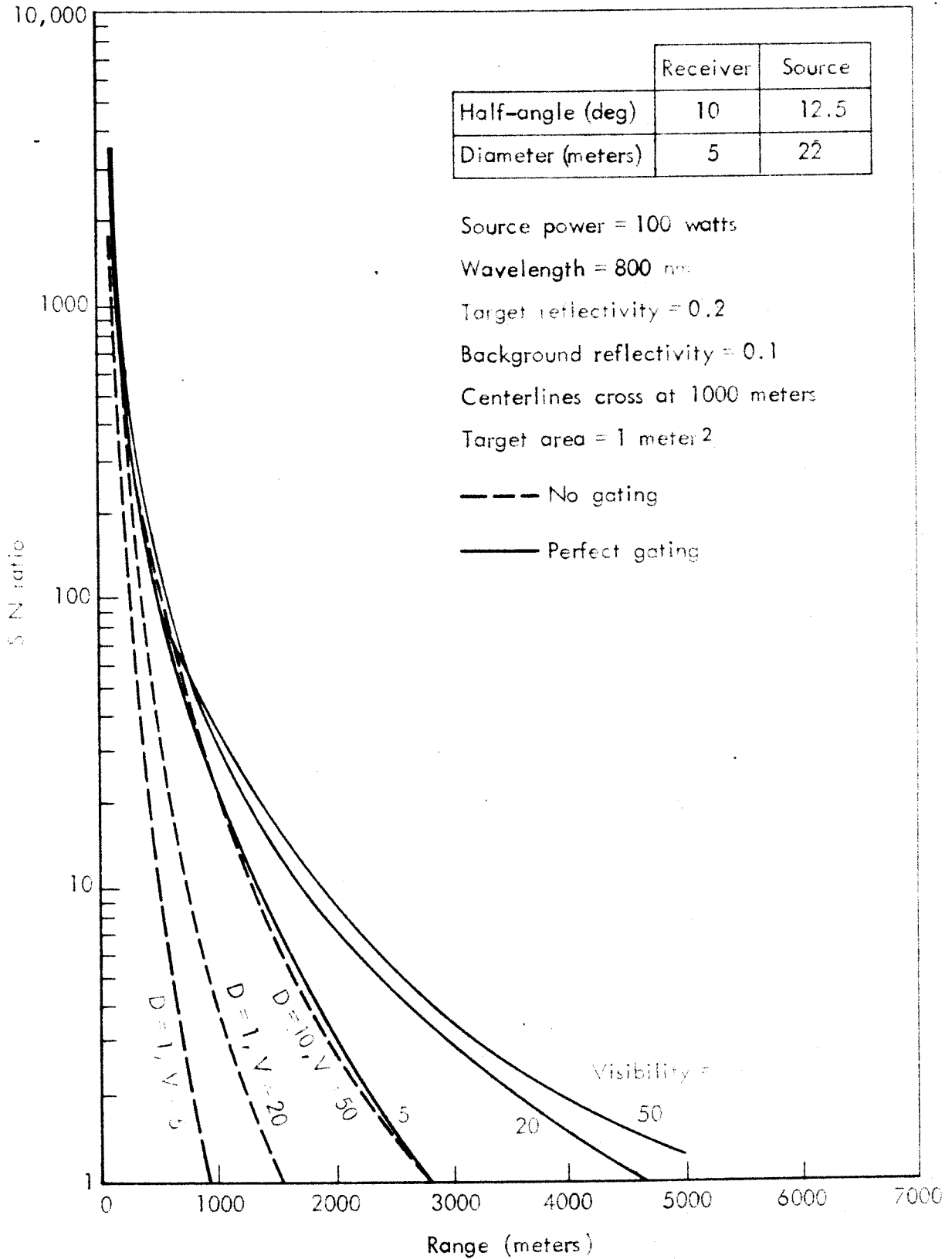


Fig. 8—S/N characteristics of General Purpose System ($\lambda = 800 \text{ nm}$)

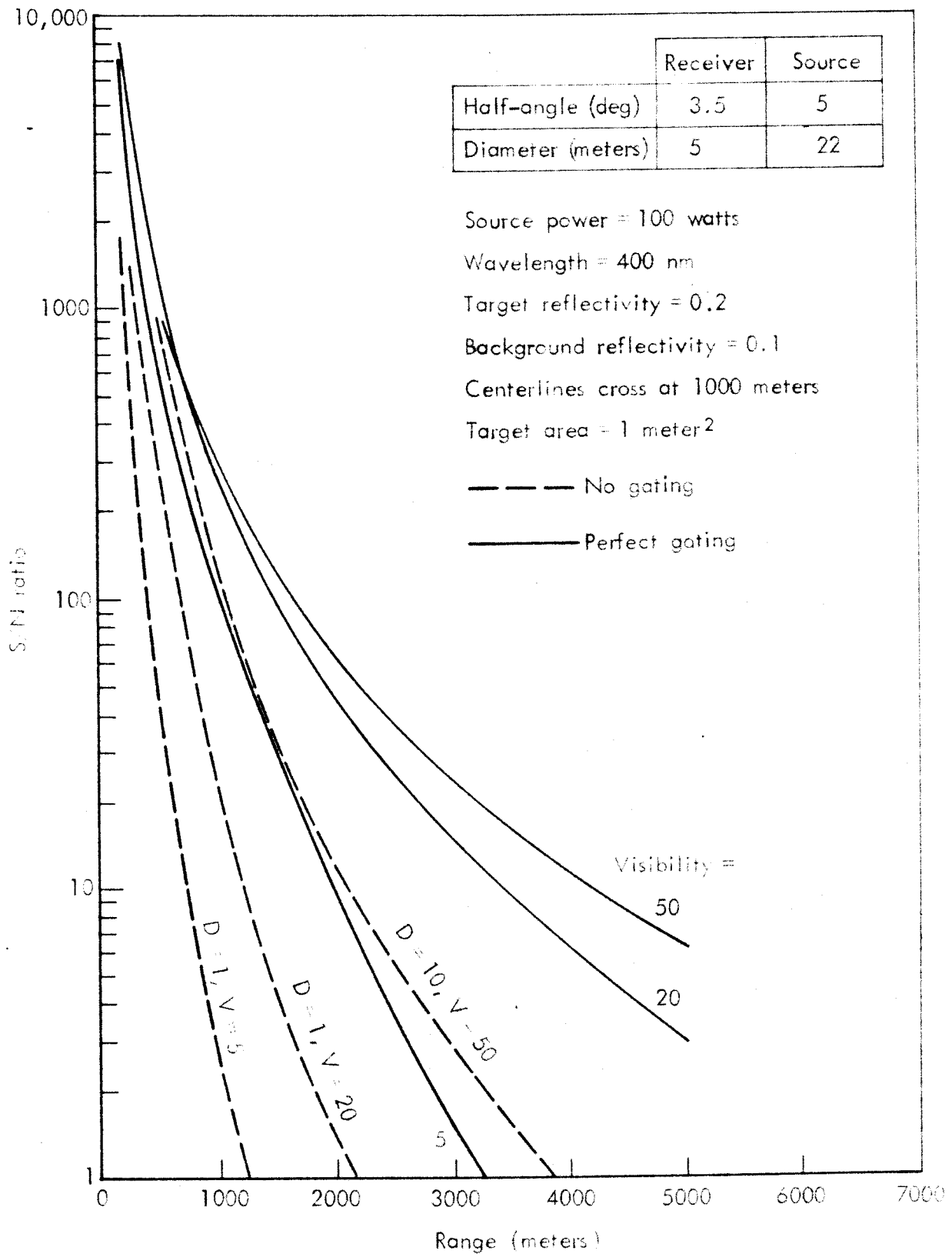


Fig. 9—S/N characteristics of Intermediate System ($\lambda = 400 \text{ nm}$)

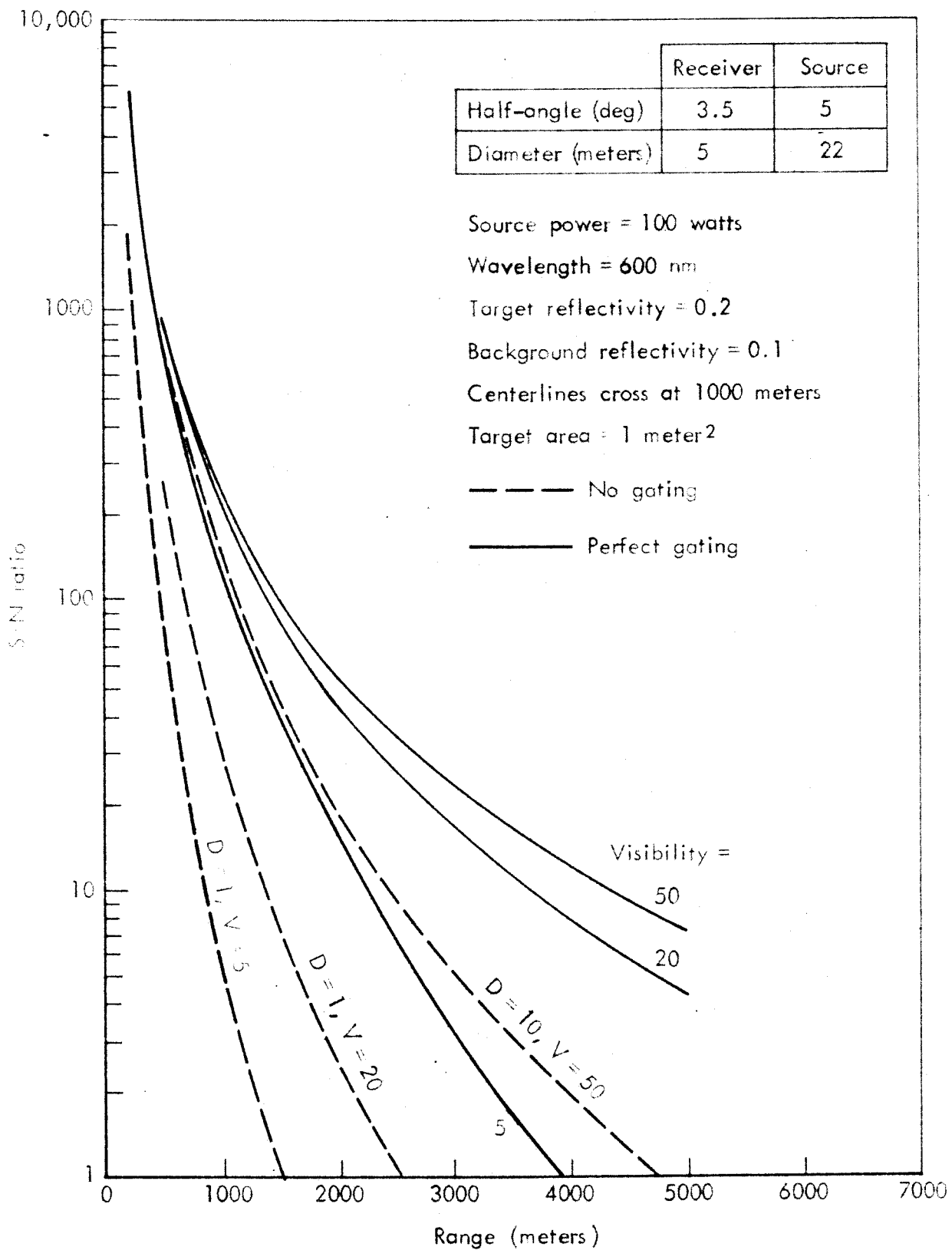


Fig. 10—S/N characteristics of Intermediate System ($\lambda = 600 \text{ nm}$)

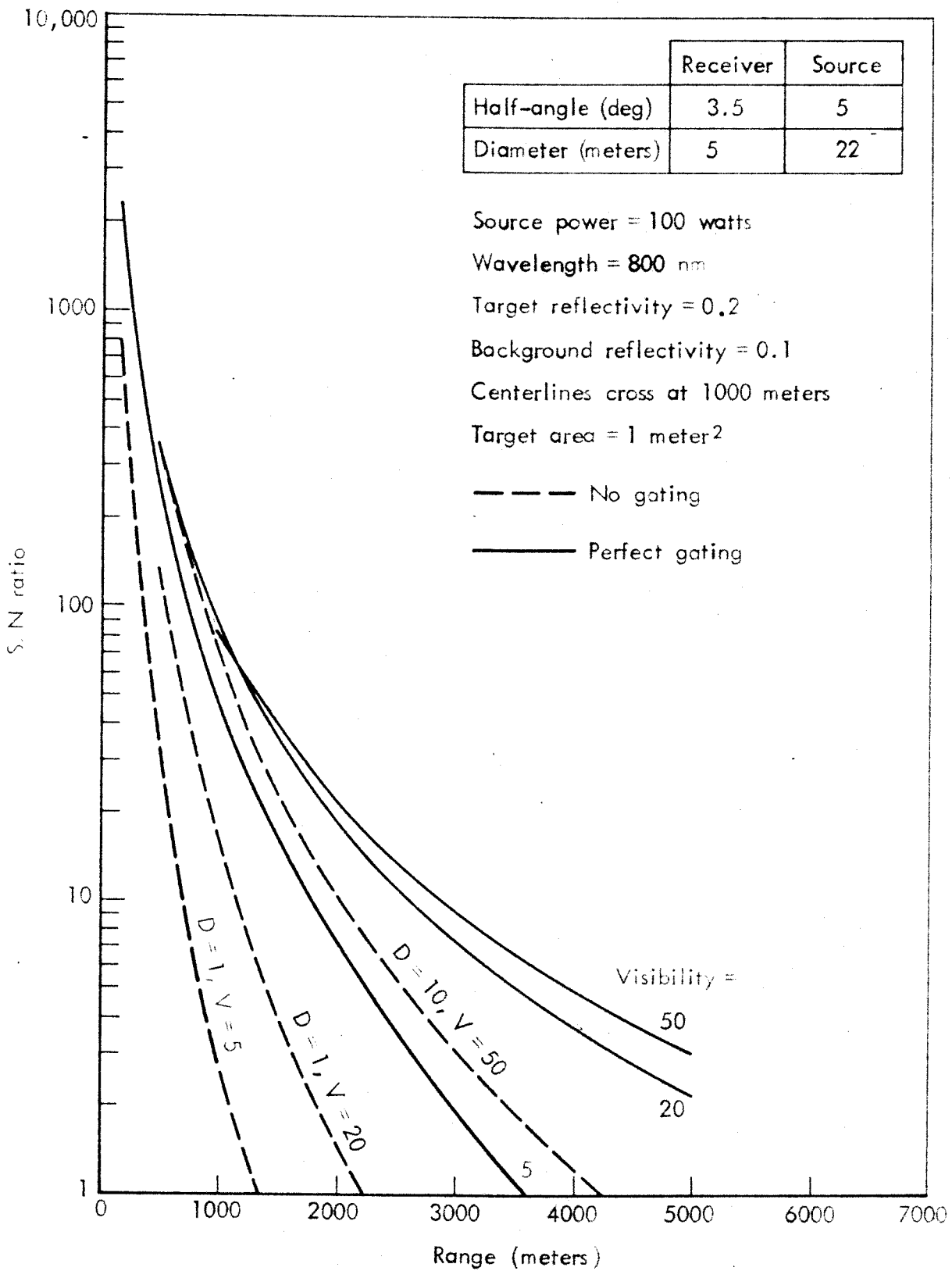


Fig. 11—S/N characteristics of Intermediate System ($\lambda = 800 \text{ nm}$)

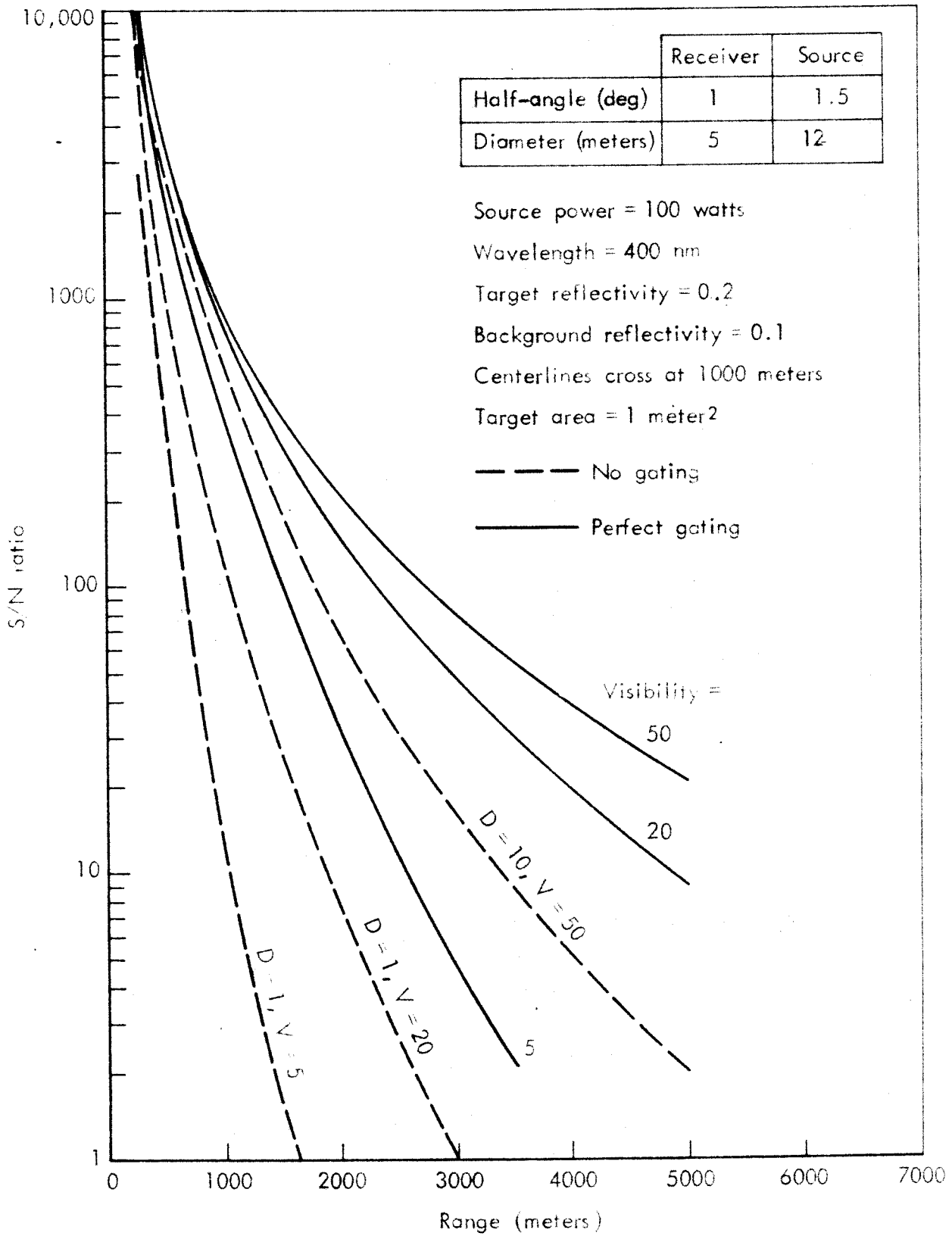


Fig. 12—Narrow Angle System ($\lambda = 400 \text{ nm}$)

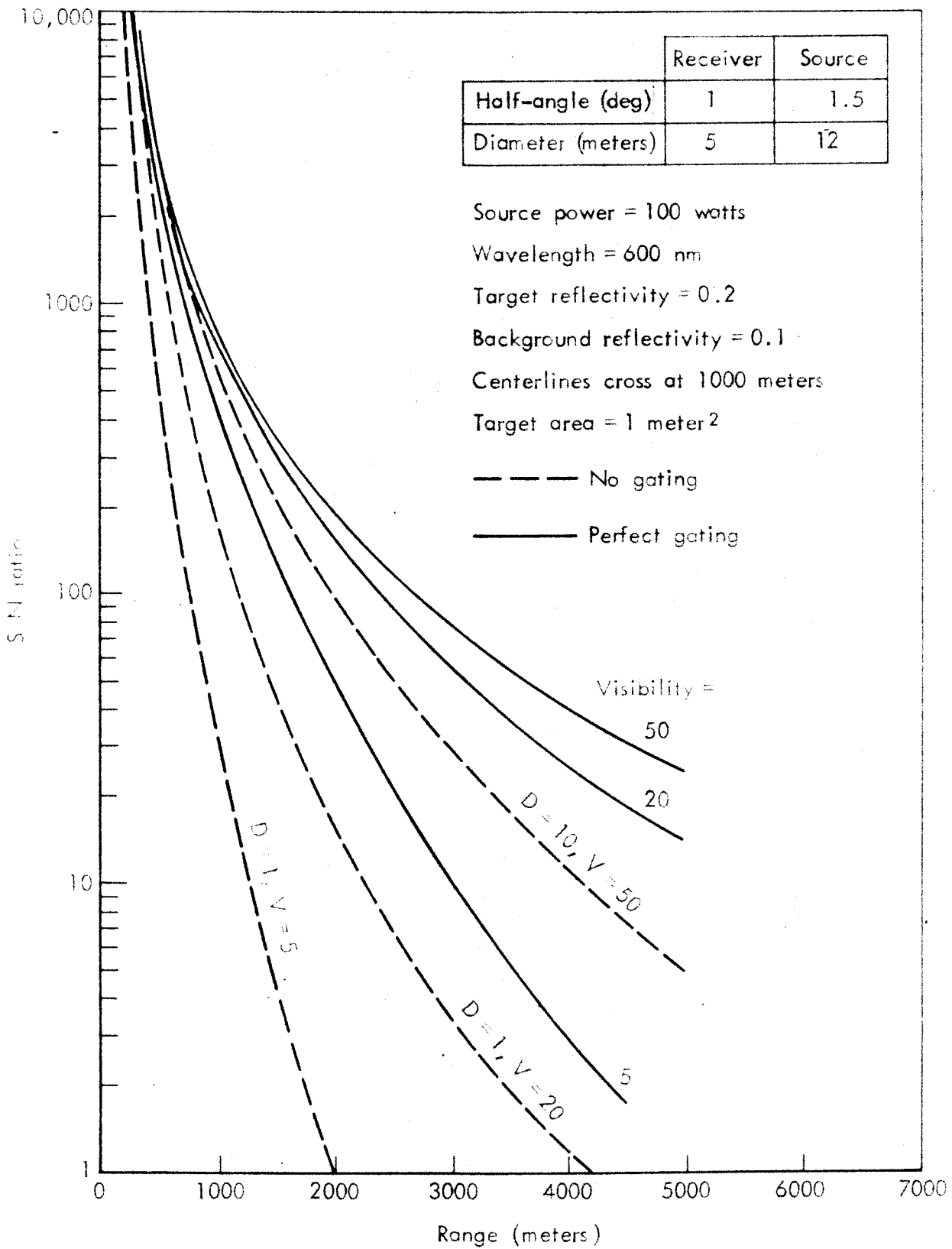


Fig. 13—Narrow Angle System ($\lambda = 600 \text{ nm}$)

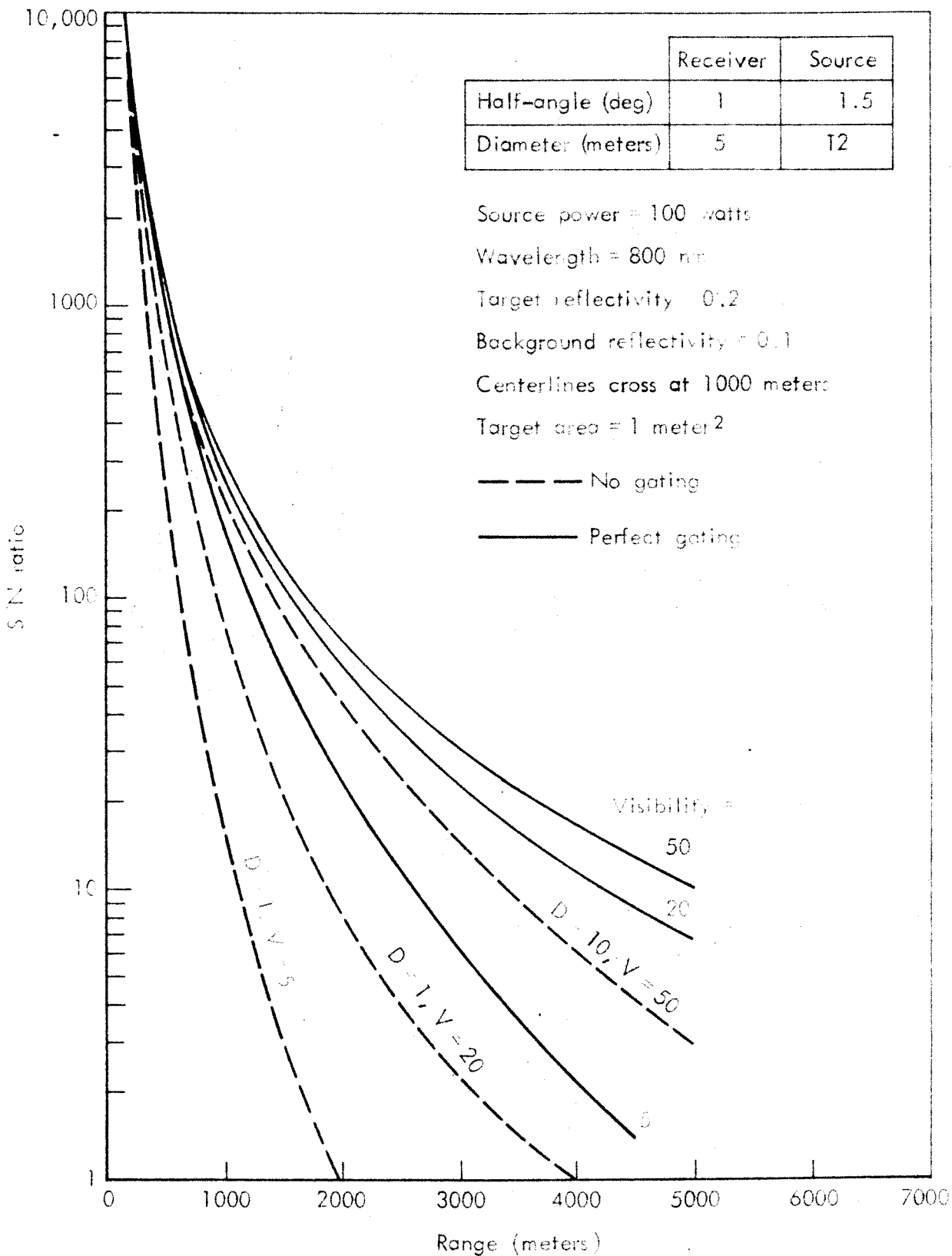


Fig. 14—Narrow Angle System ($\lambda = 800 \text{ nm}$)

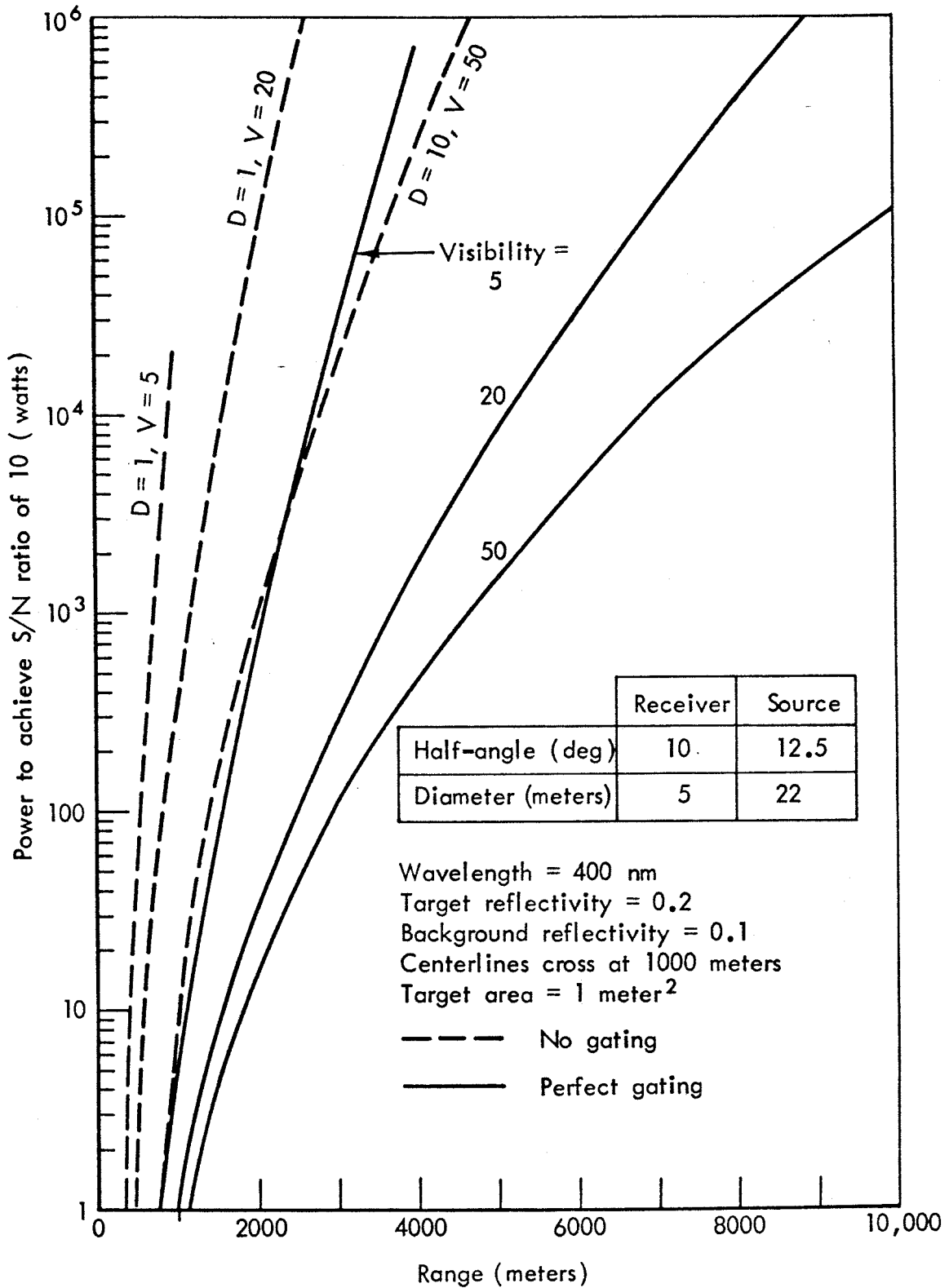


Fig. 15—Power required of General Purpose System
($\lambda = 400$ nm)

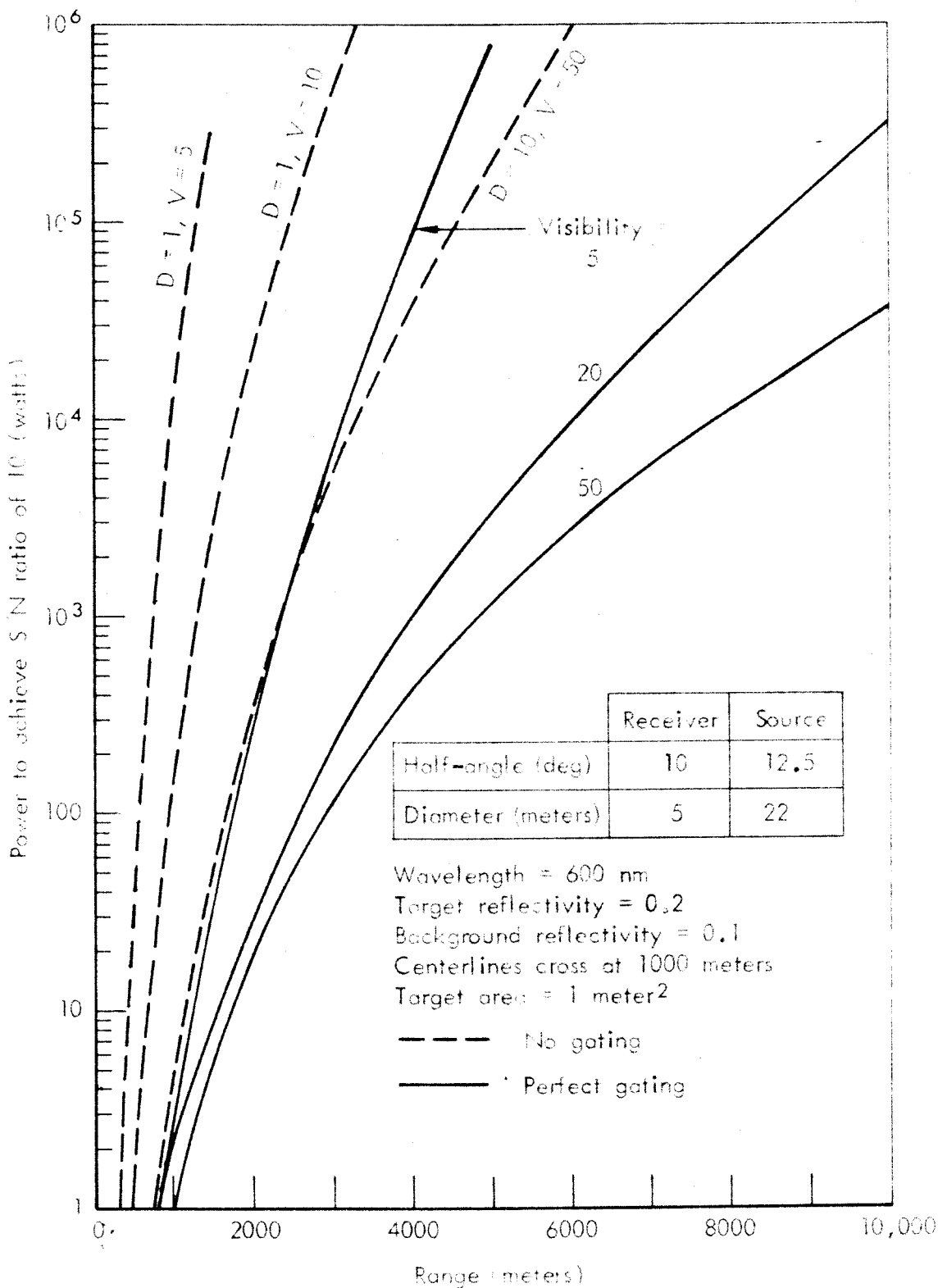


Fig. 16—Power required of General Purpose System
 ($\lambda = 600 \text{ nm}$)

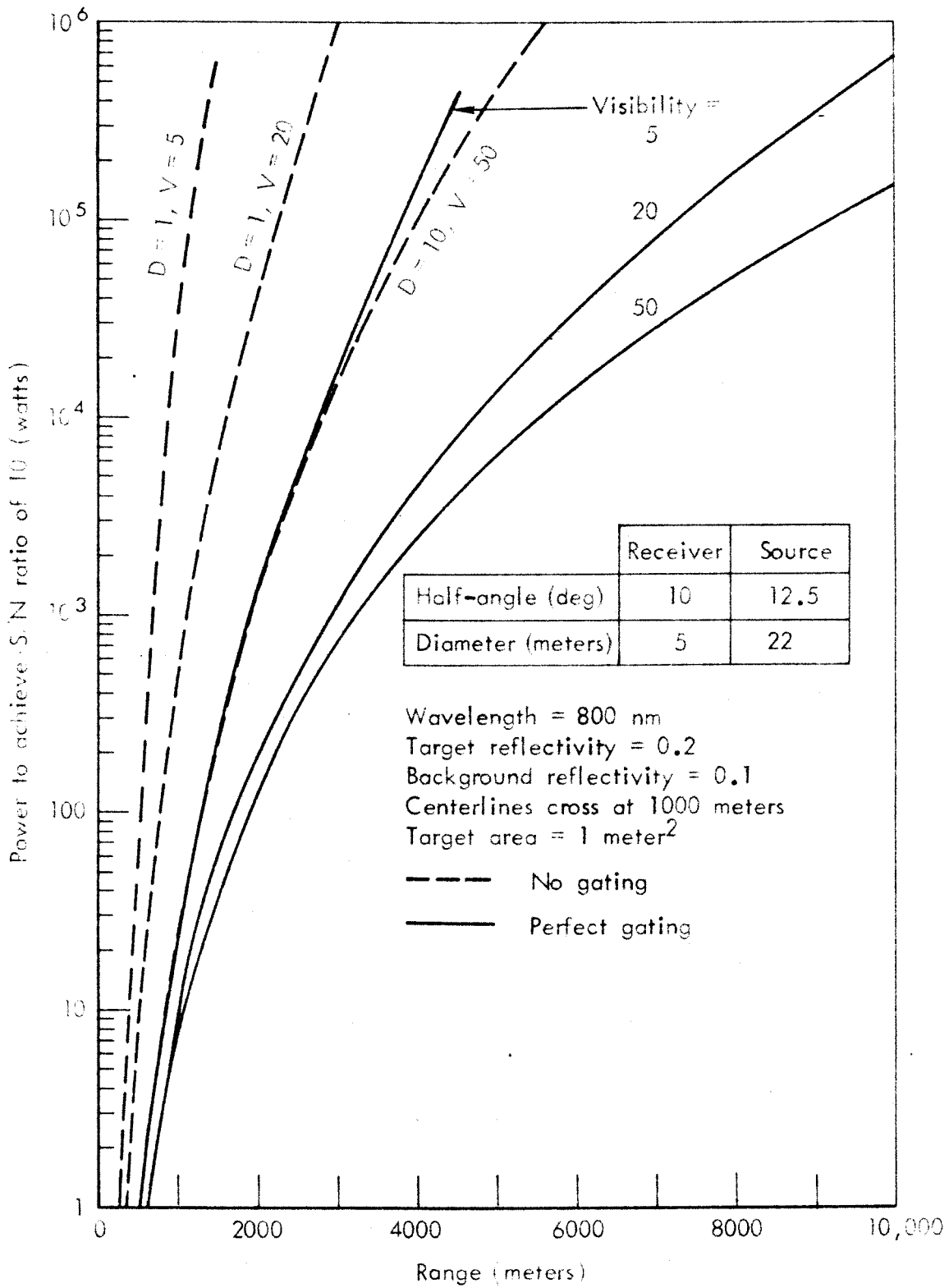


Fig. 17— Power required of general purpose system
($\lambda = 800$ nm)

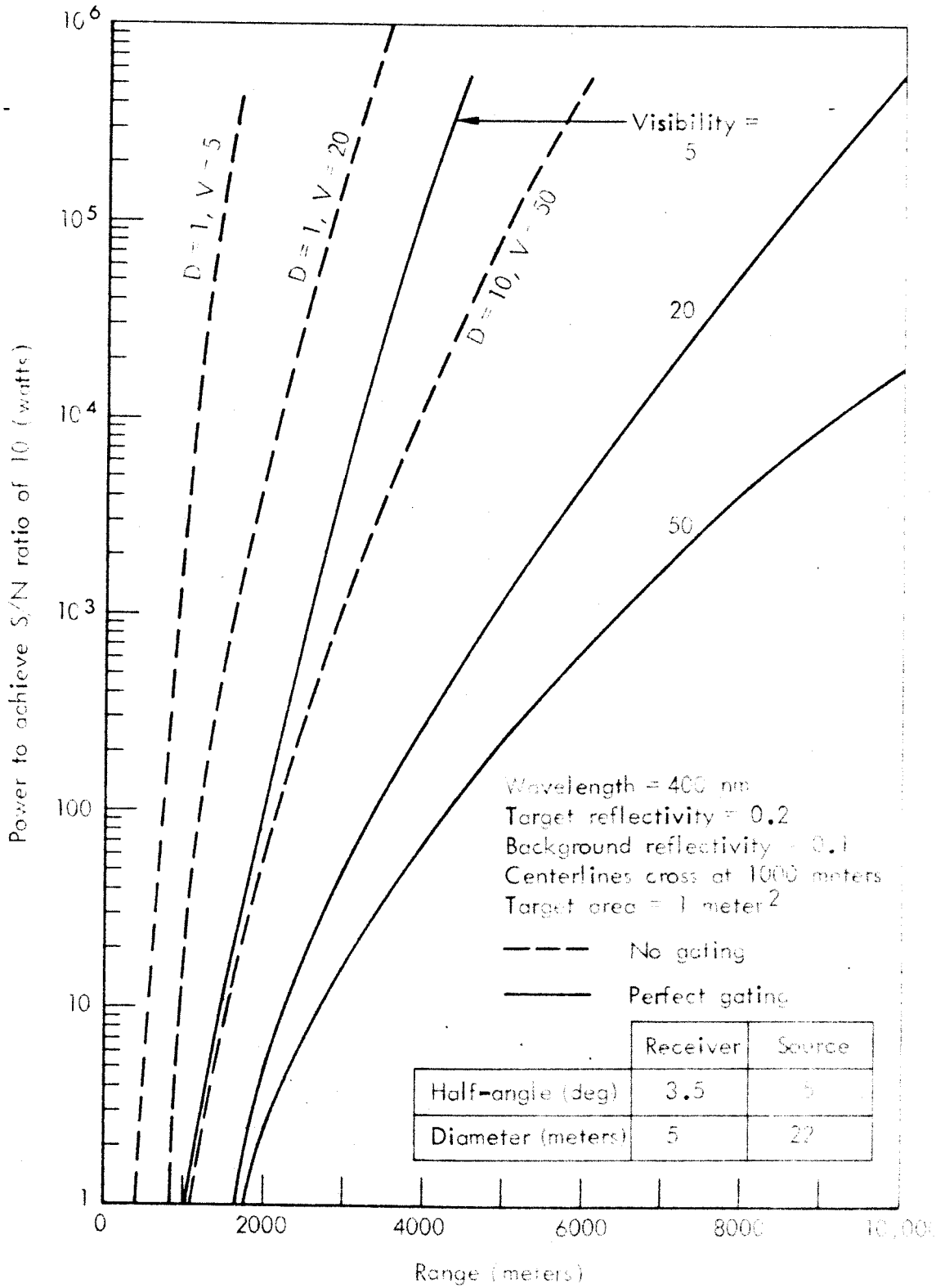


Fig. 18— Power required of intermediate system
 ($\lambda = 400 \text{ nm}$)

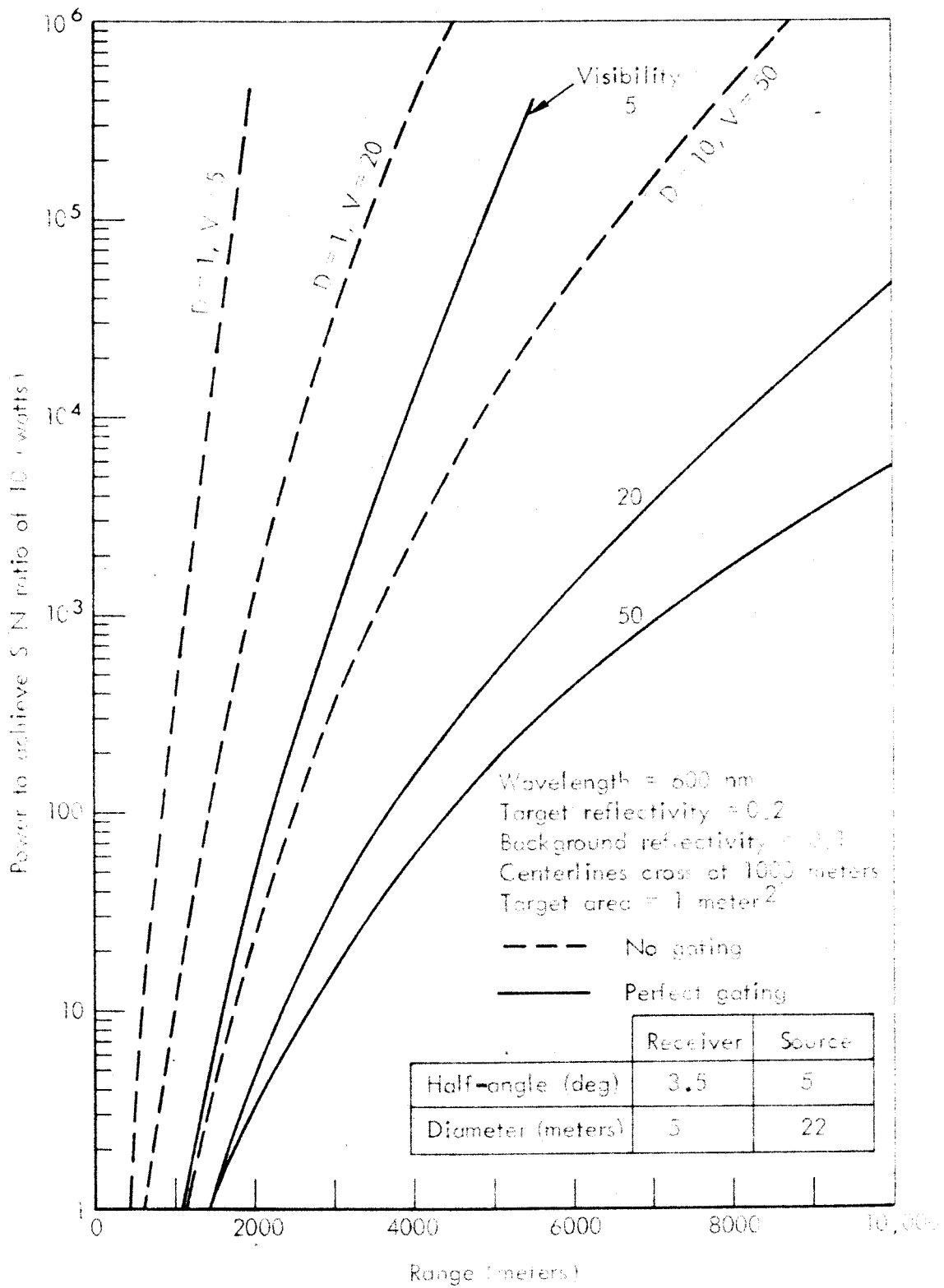


Fig. 19—Power required of intermediate system
 ($\lambda = 600 \text{ nm}$)

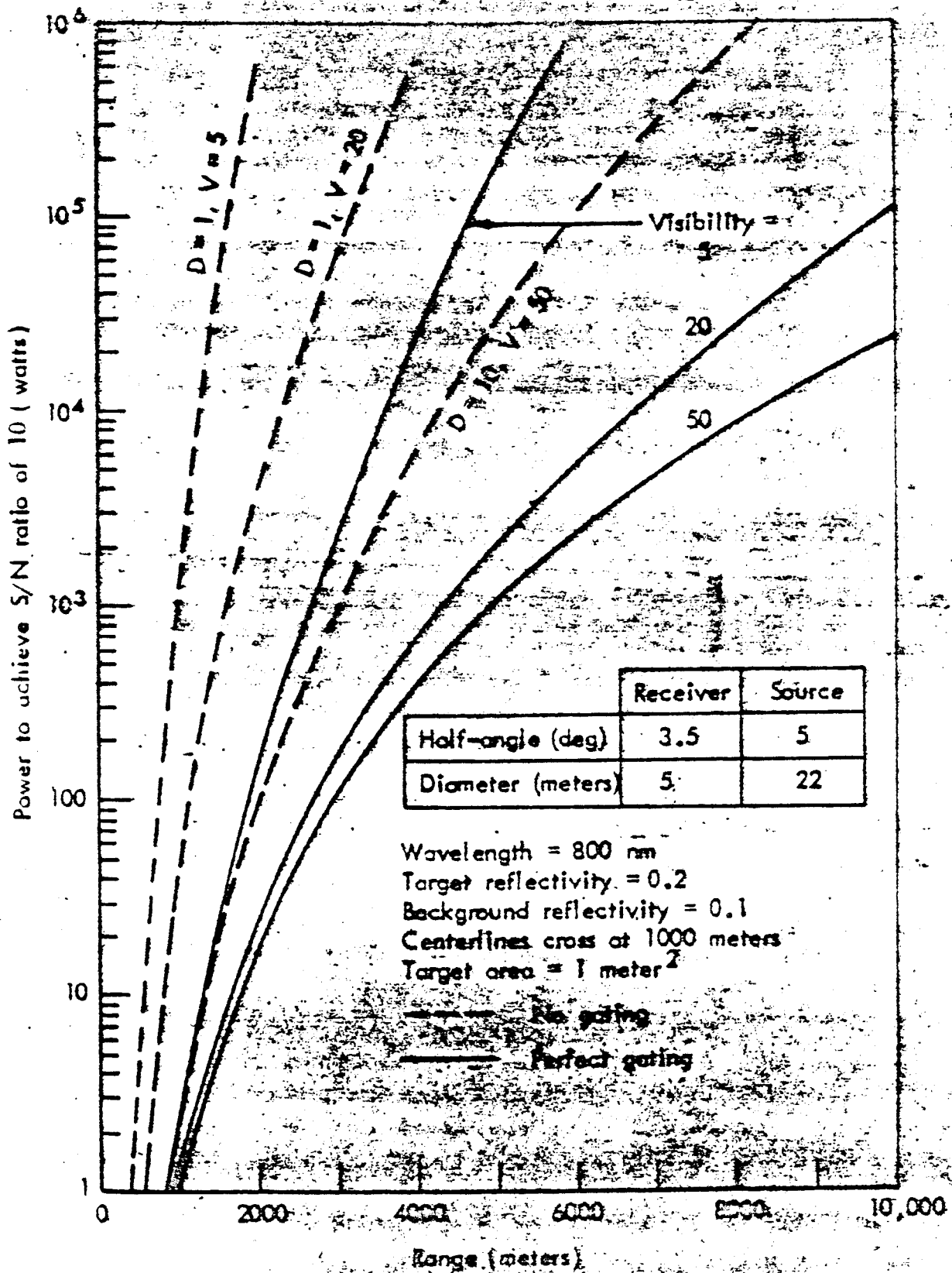


Fig. 20—Power required of intermediate system
($\lambda = 800 \text{ nm}$)

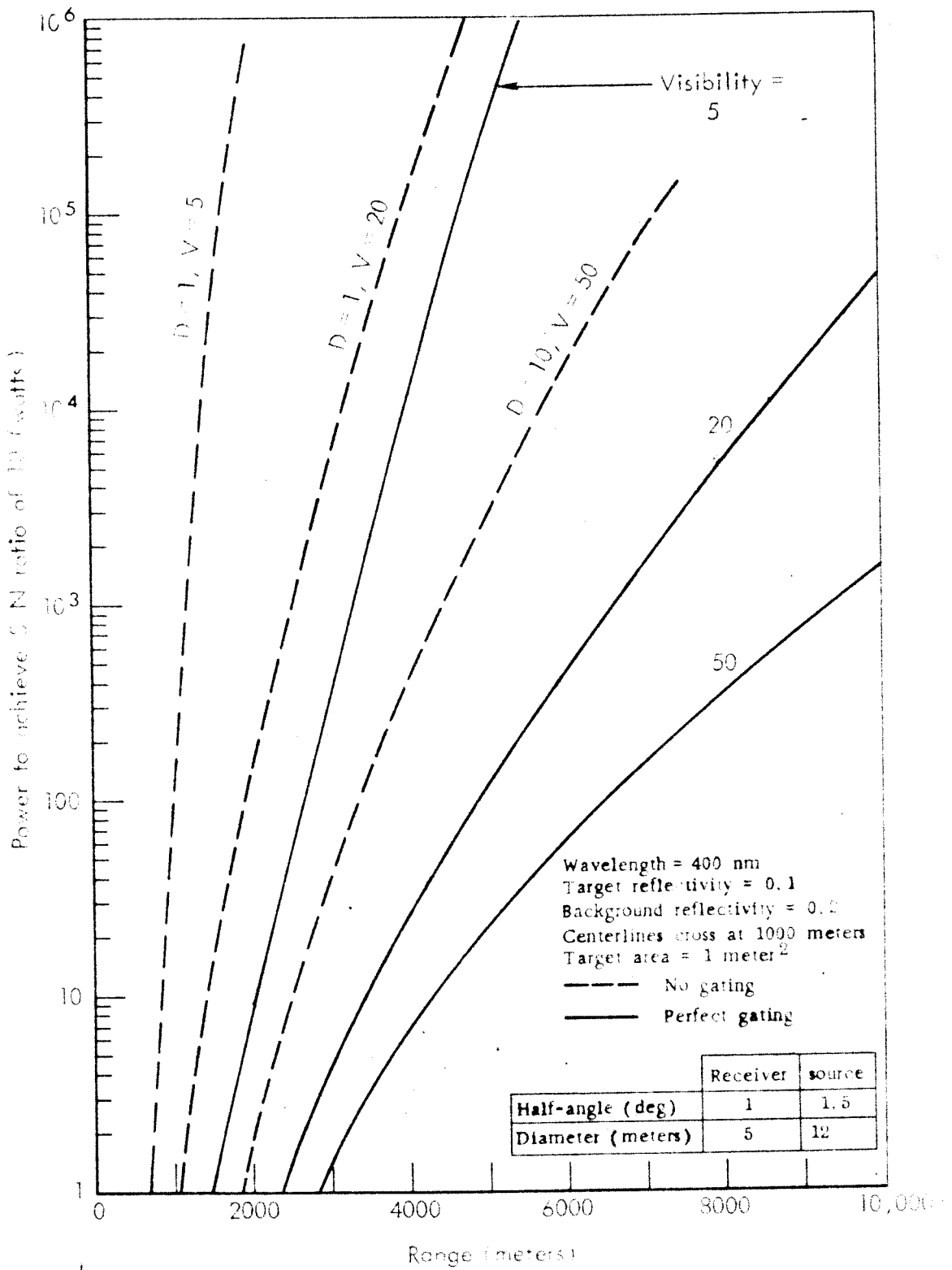


Fig. 21—Power required of narrow angle system
 ($\lambda = 400 \text{ nm}$)

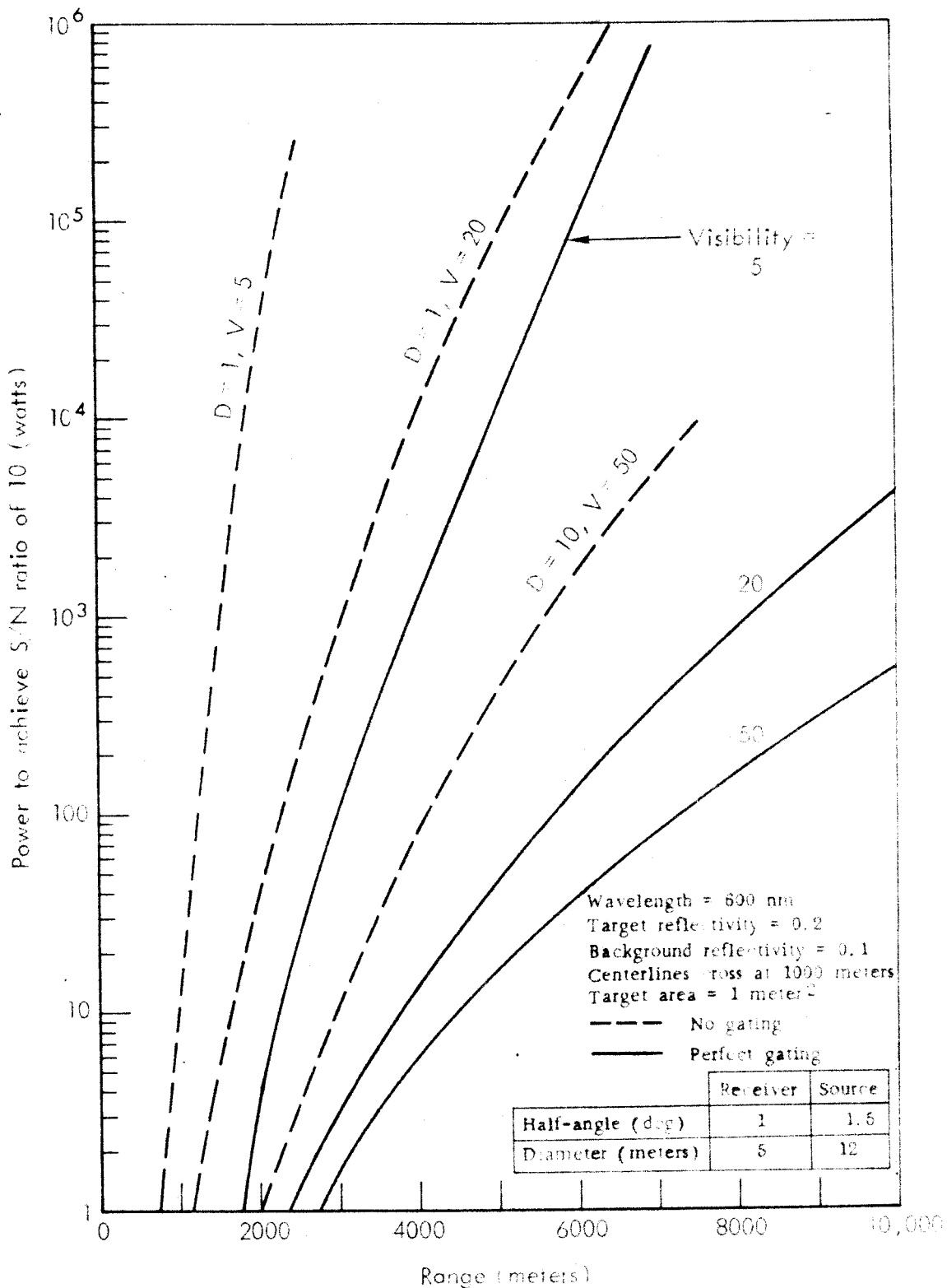


Fig. 22—Power required of narrow angle system
 ($\lambda = 600 \text{ nm}$)

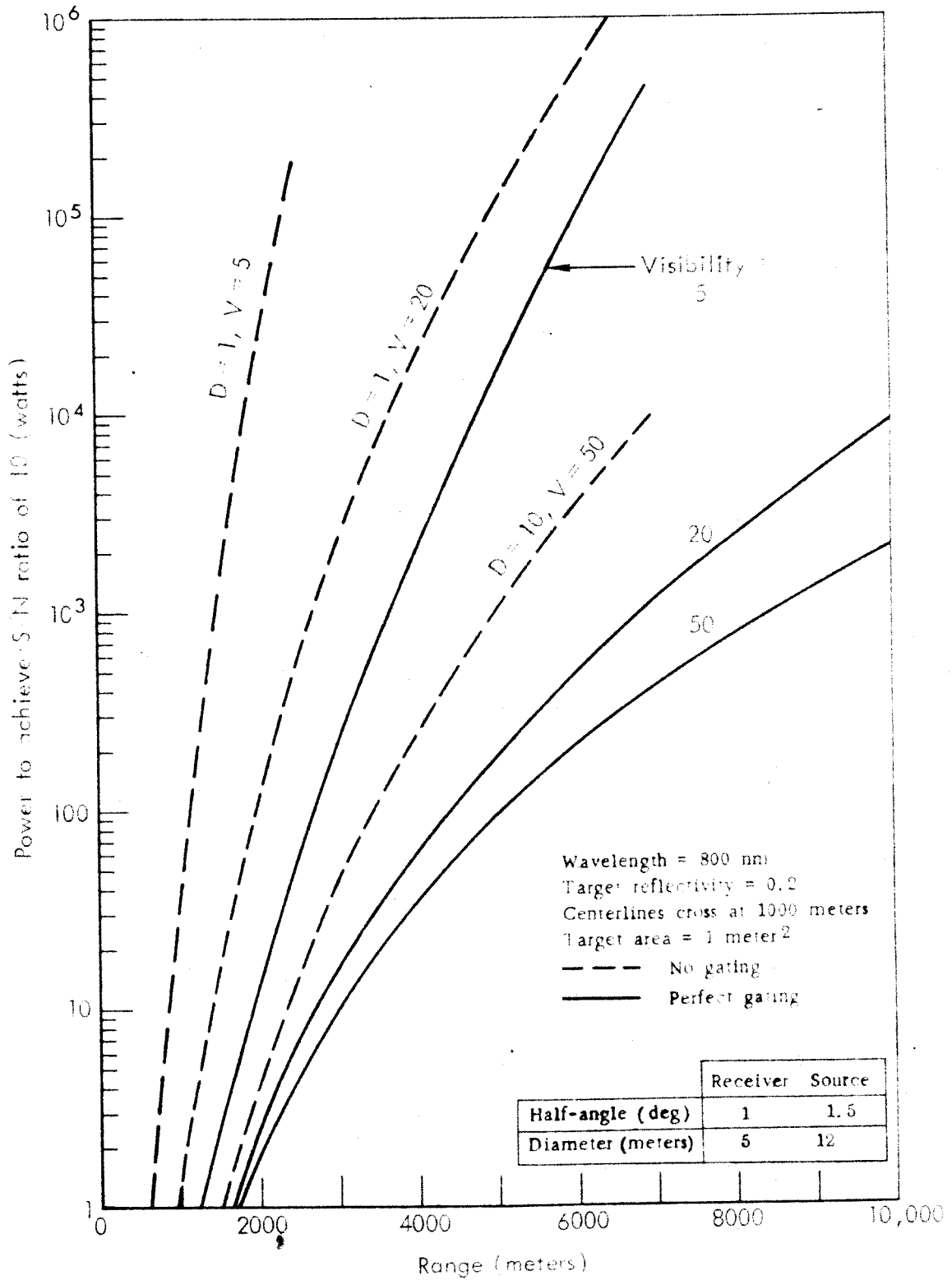


Fig. 23—Power required of narrow angle system
 ($\lambda = 800 \text{ nm}$)

REFERENCES

1. Mood, A., Introduction to the Theory of Statistics, McGraw-Hill Book Co., Inc., New York, 1950.
2. Rose, A., "Television Pickup Tubes and the Problem of Vision," Advances in Electronics, Vol. 1, Academic Press, 1958, pp. 131-166.
3. RCA Multiplier Phototubes PIT-701, Radio Corporation of America, Harrison, New Jersey.
4. Kruse, P. W., L. D. McGlauchlin, and R. B. McQuistan, Elements of Infrared Technology: Generation, Transmission, and Detection, John Wiley and Sons, Inc., New York, 1962.